ISSN 1016-3115

wgn

22 - 4
august 1994

bimonthly journal of the international meteor organization

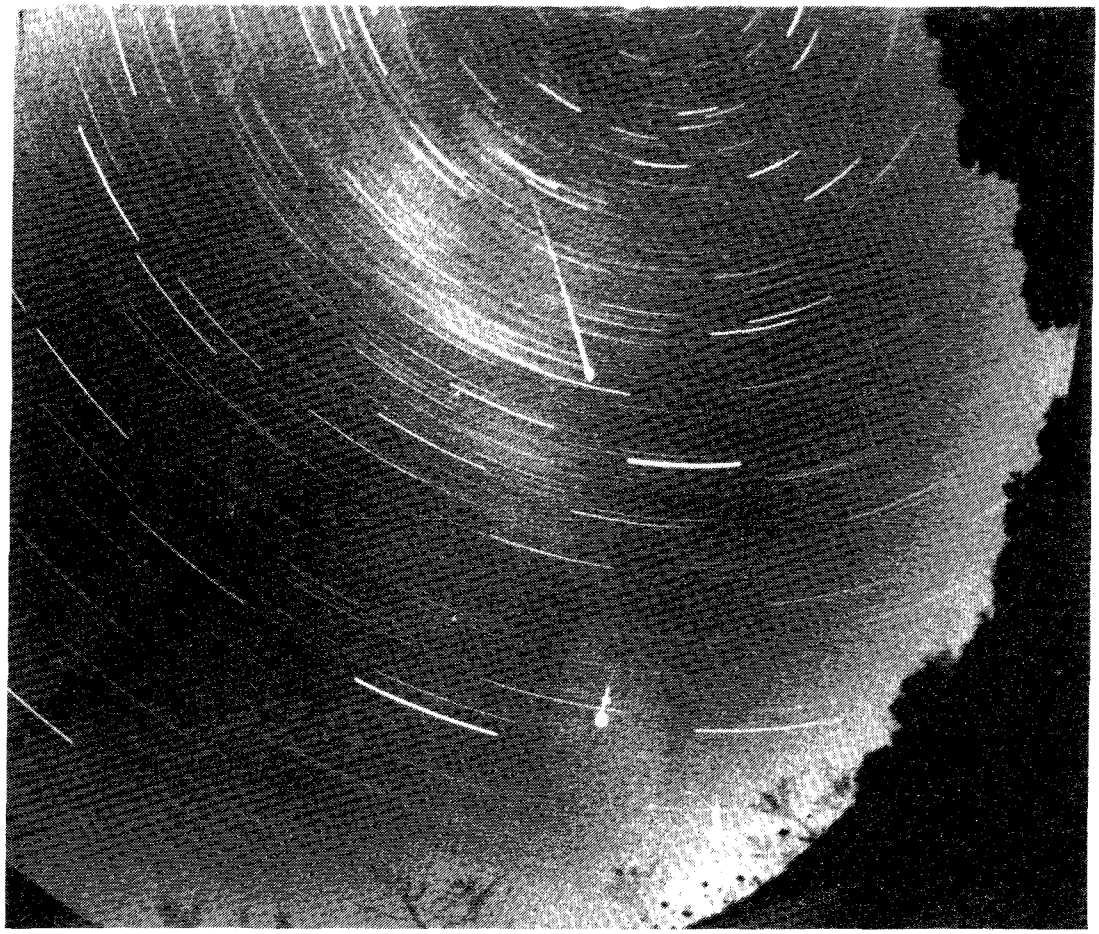

Fish-eye photograph (8 mm Nikkors) made from Salernes, France in the early morning of August 12, 1993, by members of the *Dutch Meteor Section*. The magnitude −6 Perseid ended with a terminal burst near the head of Draco at $0^h02^m47^s$ UT. The short but strongly flairing trail west of the Summer Triangle belongs to a −8 κ-Cygnid which appeared at $0^h34^m52^s$. More on this and other photographs elsewhere in this issue.

In this issue:

In case of non-delivery, return postage guaranteed. Please return to:
v.u.: Marc Gyssens, Heerbaan 74, B-2530 Boechout, Belgium

WGN, Vol. 22, No. 4, August 1994, pp. 105–154

Contents

Useful Information

The October Issue *(WGN 22:5)*

The *October issue* will be mailed during the second week of October. Contributions are due *September 25* at the latest. They should be sent to *Marc Gyssens*.

WGN Subscription/IMO Membership 1994

The subscription rate for Volume 22 (1994) of the *Bimonthly Journal* is 25 DEM for six issues which are anticipated to contain over 250 pages in total. A combined subscription with the *Report Series* and *FIDAC News* costs 60 DEM. You can also become a Supporting Member by paying at least 15 DEM extra.

From the Editor-in-Chief

Marc Gyssens

First of all, my apologies for the delay in bringing out this issue. Several mostly personal items interfered with the preparation of the August issue. I have good hopes, however, that we will be back on schedule this fall.

Again, the Perseids showed an outburst, witnessed mainly from the North-American West Coast. A preliminary report on this year's performance of the Perseids is included in this issue.

Finally, people still wishing to participate in the 1994 IMC, *but who could not previously commit themselves, probably still can do so, provided they contact the organizers* immediately *upon receipt of this issue. (See also the notice below.) Meanwhile, enjoy this issue!*

The 1994 International Meteor Conference

Belogradchik, Bulgaria, September 22–25

Valentin Velkov, Eva Bojurova, and Zahari Donchev

The *International Meteor Conference* in 1994 will take place in the small, very old historical town of Belogradchik, Bulgaria. What made us select this place for the *IMC* in our country is the extraordinary combination of an amazing natural phenomenon—the Belogradchik Rocks, a historical monument—ancient fortifications of the 13th century, and a professional astronomical observatory—one of the two observatories of the Bulgarian Academy of Science. All these features are very close to each other and within walking distance from the town center. They will be visited during the traditional excursion on the third day of the conference.

People who wish to participate, but have not yet registered can phone or write to us *immediately after receiving this issue*. Probably we can still arrange something for them. The address is *Astronomical Observatory and Planetarium N. Copernicus, P.O. Box 120, BG-9000 Varna, Bulgaria*, telephone +359-52-222890.

Letters for WGN

compiled by Marc Gyssens

On a lighter note

*In the previous issue, Rainer Arlt suggested to use a cash register roll to write down Perseid observations efficiently (*WGN *22:3, pp. 87–88). Our Maltese friends took his suggestions even further...*

Rainer Arlt's article in *WGN* 22:3 on "Hints for visual observations of the Perseids" has generated a humorous twist among meteor watchers in Malta. A preparatory meeting of the *Astronomical Society Meteor Group* duly proceeded to inform Maltese prospective Perseid observers of the techniques suggested in Rainer Arlt's article, particularly for use during high-ZHR events. We have designated these techniques WART (Watching Activity with Rapid Techniques)—knowing that suggestive names help one's memory and act as a pleasant diversion to serious issues. The suggestion was made that one alternative to the paper roll (on which observers are to write blindly to avoid dead time) is, apart from cash register roll, a toilet paper roll. This is much more easily available, cheaper and more voluminous.

Five members proposed to carry out a pilot study of the suitability of toilet paper to WART, testing the capacity of two different brands—one soft; one hard—in typical observing conditions. I enclose a copy of their "scientific result" plus "samples". I have, in the meantime, earned the not-so-glorious title of "Official Toilet Paper Consultant." Perhaps the toilet roll was not such a good idea after all?!

Godfrey Baldacchino, August 1, 1994

Unfortunately, we cannot reproduce the "samples." The "scientific results" follow below.

Dear Godfrey,

Enclosed please find our trail observations using the WART method. We hope that you, the Society, and the *IMO* find these observations worthy in deciding which is the best branch of toilet paper to be used for this summer Perseid project.

These are our findings:

- *Toilet paper 1*: Was found to be soft and easy to handle, not so good to green observers. In windy conditions, it can easily break . Also in dew it can get easily wet.
- *Toilet paper 2*: Hard, rough, but resistant. Good for bad weather, the only problem is that it is too white; it may easily hamper your dark adaption. Not so good for its original use.

We look forward to an early reply and comments so that we can invest in the right stuff.

Bernard, Antione, Mark, Adrian, Franco

Frequently Asked Questions on Observing Methods

compiled by Rainer Arlt

Is the radiant drift given in the Shower Calendar relevant for my observation?

Yes, definitely. Geometrical reasons cause a radiant motion of each shower. The drift is nearly parallel to the ecliptic. Hence, ecliptical showers have the largest radiant motion and those near the ecliptical pole have very small drifts (e.g., κ-Cygnids, Ursids, α-Carinids) which are neglectable.

There are additional tables for the radiant motion for showers with long activity periods in the Calendar. Never use the radiant positions given in the main table for these showers. The radiant positions of the other showers can be calculated from the difference in days between the date of observation and the date of maximum. If you observe before the maximum this difference is negative, if you watch after the maximum, the difference is positive. Let us call this difference n. Now we can calculate the radiant position with $\alpha_{new} = \alpha + n \times \Delta\alpha$ and $\delta_{new} = \delta + n \times \Delta\delta$. The variables used are the same as in the shower list of the Shower Calendar. The coordinates α and δ refer to the date of maximum. These calculations need not be too sophisticated. An accuracy of 1° is sufficient. Remember that radiant diameters are much larger. The radiant position must also be determined when you are going to observe with the counting method only.

How to convert local time into Universal Time (UT)?

Universal Time is the local time valid for 0° geographical longitude. The globe is divided into time zones. Each country has one or more time zones with a fixed difference to UT in hours. If your country uses daylight-saving time during the summer months, this difference changes by one hour. The following table shows the difference for a number of countries. Add/subtract the given values to/from your local time.

Table 1 – Convertion of local time zones in Universal Time. The column "St.T." gives the normal time difference to UT, the "D.S.T." gives the difference for daylight-saving-time periods

Country	St.T.	D.S.T.	Country	St.T.	D.S.T.
Australia			Pakistan	− 5	− 6
WAST/WADT	− 8	− 9	Portugal	− 1	− 2
Austria	− 1	− 2	Rumania	− 2	− 3
Benelux	− 1	− 2	Slovakia	− 1	− 2
Bulgaria	− 2	− 3	Slovenia	− 1	− 2
China	− 8	− 9	South Africa	− 2	− 3
Croatia	− 1	− 2	Spain	− 1	− 2
Czech Republic	− 1	− 2	Sweden	− 1	− 2
Finland	− 2	− 3	United Kingdom	0	− 1
France	− 1	− 2	Ukraine	− 3	− 4
Germany	− 1	− 2	USA/Canada		
Hungary	− 1	− 2	AST/ADT	+ 4	+ 3
Italy	− 1	− 2	EST/EDT	+ 5	+ 4
Japan	− 9	−10	CST/CDT	+ 6	+ 5
Jordan	− 2	− 3	MST/MDT	+ 7	+ 6
Malta	− 1	− 2	PST/PDT	+ 8	+ 7
New Zealand	−12	−13	Hawaii ST	+10	
Norway	− 1	− 2	Yugoslavia	− 1	− 2

If you are not sure how to convert your times into UT, please note on your report explicitly which time you used. Be also very careful that the date may change when you convert your local time into UT.

The Meteor Train Observing Project in 1993

Mark Vints

1. Status report of the observing project

As of June 1, 1994, the following observers have submitted train reports for their 1993 observations. Included between brackets is the number of reports received from each.

Rainer Arlt (1), Neil Bone (8), Gert Bonné (1), Lieve Bresseleers (3), Steven Broos (1), Natasja Brughmans (1), Tom Buerms (1), Sabine Clement (1), Eric Crauwels (2), Albert De Clerck (1), Roel Derickx (1), Atanas Dimitrov (2), Michael Funke (1), Shelagh Godwin (3), Ivan Goethals (1), Erwin Guetens (1), Udo Hennig (1), Kathleen Hermans (3), Wolfgang Hinz (2), Danielle Hoja (1), David Holman (8), Andreas Krawietz (4), Rhena Krawietz (4), Holger Lau (1), Richard Livingstone (9), Robert Lunsford (29), Stefan Meister (2), Frank Melillo (2), Alastair McBeath (13), Tom McEwan (1), Svetoslav Minkov (2), Thomas Rattei (2), Jürgen Rendtel (15), Ian Rigney (9), Thomas Schreier (1), Thomas Scott (1), Wanda Simmons (1), Alan Smeaton (3), George Spalding (5), Siegfried Stapf (11), Dominique Suys (1), Frank Van der Spiegel (1), Pierre Van Mechelen (1), Cis Verbeeck (1), Tinne Verhaegen (1), Nancy Vermeulen (1), Thomas Voigt (6), Sabine Wächter (5), Roland Winkler (4), Vaya Willemen (1), Graham Wolf (37), George Zay (75).

Not included in this list are 51 train reports on 50 different fireball events between 1985 and 1993, submitted by Graham Wolf. Most of the reports submitted are complete and filled out correctly. Nevertheless there remains a tendency to neglect sporadic meteors and minor showers. This information, however, is just as valuable as data on major showers. Train reports from previous years remain very welcome; the report form can be found in *WGN* 21:3 (June 1993). In case of uncertainties or difficulties in completing the form, please consult me first.

The totals for 1993 now stand at 293 reports submitted by 52 observers, covering 16186 meteors seen in 1081 hours on 146 different nights. I wish to thank all participants for their observational and administrative efforts, especially those who collected and submitted results from several people. A breakdown by month is presented in Table 1. Not surprisingly, the Perseids were best covered, and this shower is presented in more detail.

Table 1 – Train observations during 1993.

Month	Days	Rep.	Nr. Obs.	T_{eff}	Met.	Trains
Jan	6	13	7	54.71	532	60
Feb	7	7	3	28.73	83	12
Mar	17	19	4	76.26	280	20
Apr	12	14	3	75.11	505	55
May	7	11	4	46.86	194	16
Jun	15	20	5	69.47	209	17
Jul	18	30	8	121.86	1159	145
Aug	17	110	48	335.14	8583	2229
Sep	6	6	3	28.77	213	23
Oct	20	31	8	97.01	1202	226
Nov	14	18	8	70.55	504	82
Dec	7	14	7	76.93	2704	154
Tot	146	293	52	1081.40	16168	3039

2. A case study of the 1993 Perseids

Given the good coverage of the Perseid shower in 1993, it is worthwhile to look deeper into the train reports received. An analysis was carried out on 5138 Perseids and 1797 sporadic meteors reported by 48 observers in the US and Europe between August 7-8 and 15-16. In my opinion, the sample size did not allow a reliable day-by-day analysis, so all observations were taken together initially. Tables 2 and 3 summarize the result, and show for each of several magnitude classes the number of meteors and trains seen, the percentage of meteors showing a train, and the average train duration in seconds.

Table 2 – Magnitude and train distributions for the 1993 Perseids.

Magnitude	-6^-	$-5/-4$	$-3/-2$	$-1/0$	$+1/+2$	$+3/+4$	$+5/+6$	Tot
Meteors	29	67	223	916	2062	1616	225	5138
Trains	25	54	181	539	779	197	14	1789
% Trains	86	81	81	59	38	12	6	35
Duration (^{s})	22	9	3.4	1.7	1.0	0.7	0.5	2.0

Table 3 – Magnitude and train distributions for the corresponding sporadics.

Magnitude	-2^-	$-1/0$	$+1/+2$	$+3/+4$	$+5/+6$	Tot
Meteors	24	179	556	875	163	1797
Trains	9	46	94	47	12	208
% Trains	38	26	17	5	7	12
Duration (s)	2.7	2.1	1.1	0.9	0.5	1.3

In comparing Perseid and sporadic meteors within the same magnitude class, it is seen that roughly twice as many Perseids show a train, while the average train duration remains about the same. Overall, the train percentage for the Perseids is 3 times as high as that for the sporadics, which is not surprising given the fact that they are on average a full magnitude brighter than the sporadics. Next, the analysis was confined to the observations of just 6 observers who saw a sufficiently large number of meteors under good atmospheric conditions. These obervers are Rainer Arlt, David Holman, Alastair McBeath, Jürgen Rendtel, Siegfried Stapf, and George Zay. Tables 4 and 5 are as the previous ones, but this time comparing the complete set from these 6 observers with their results for August 11-12 only.

Table 4 – Magnitude and train distributions for the 1993 Perseids for the selected group of observers.

Magnitude	-6^-	$-5/-4$	$-3/-2$	$-1/0$	$+1/+2$	$+3/+4$	$+5/+6$	Tot
Meteors	17	37	130	465	961	665	107	2382
Trains	16	30	108	308	390	53	1	906
% Trains	94	81	83	66	40	8	1	38
Duration (s)	26	10	3.4	2.1	1.2	0.8	0.5	2.5

Table 5 – Magnitude and train distributions for the Perseids on August 11-12, 1993, for the selected group of observers.

Magnitude	-6^-	$-5/-4$	$-3/-2$	$-1/0$	$+1/+2$	$+3/+4$	$+5/+6$	Tot
Meteors	12	28	86	264	564	420	72	1446
Trains	11	23	71	169	202	27	0	503
% Trains	92	82	83	64	36	6		35
Duration (s)	30	11	3.2	1.9	1.1	0.7		2.7

Tables 4 and 5 confirm the results of Tables 2 and 3 quantitatively, and demonstrate that there is no difference in the results obtained on August 11-12 and those of other nights around the maximum.

An Analysis of the Taurid Radiants

Luis R. Bellot Rubio

In 1989, the *IMO* set up the *Aquarid Project* with the main goal of finding out whether the analysis of visual data can distinguish radiants when they are rather concentrated in a given area of the sky. The results of this study [1] suggested that the separation of neighboring showers is indeed possible when a large number of meteor plots is available, they are well distributed around the radiants and certain specific tools are used. Moreover, some important data were obtained for the showers under scrutiny, namely the radiant sizes, positions and drifts.

The typical distance between radiants of the Aquarid Complex is about 10°. This is a favorable separation with respect to that of the Taurid radiants, which during some periods becomes less than 7°. As a consequence, the analysis of the Taurid Complex by means of visual data is a further step in the investigation started with the *IMO Aquarid Project*.

On the other hand, the Taurid Meteor Complex has an extreme importance, since it is believed to be the product of the decay of a very large comet. Thus, new data on its night-time showers may help to the study of such an event by imposing further constraints to theoretical models.

In particular, it was shown in [2] that up to six showers belonging to the Taurid Meteor Complex are active during September–November, the Northern and Southern Taurids being just two of them. The remaining four are the Northern Piscids, the Southern Arietids and the Northern and Southern χ-Orionids. Very little attention has been paid to these showers, as a consequence of which our knowledge of their behavior is rather incomplete.

Bearing in mind these considerations, it seems interesting to analyze the Taurid Complex with visual techniques. Unfortunately, the activity of the main showers of the Taurid Complex is very low, which means that few Taurids are seen during the night. In addition, the number of active observers diminishes in the fall, thus imposing a further limitation. Therefore, observers are asked to pay special attention to the Taurids in 1994.

Up to now, 2750 meteor plots are already available in September-end November. Table 1 gives the meteor numbers per period stored in *PosDat*, the Positional Database of the IMO. The contributing observers are listed in Table 2.

Table 1 – Meteor numbers per period.

Interval	Meteors	Interval	Meteors
Sep 01–10	53	Oct 21–31	783
11–20	235	Nov 01–10	127
21–30	48	11–20	238
Oct 01–10	198	21–30	121
11–20	947	Tot	2750

Table 2 – Contributing observers.

Observer	Met.	Observer	Met.	Observer	Met.	Observer	Met.
Rainer Arlt	200	Mario Gaitano	3	A.R. Paños	1	A. Román	13
Luis Bellot	187	V. González	2	E. Ortega	12	Á. Rute	4
J. Caballero	2	S. Guntez	1	J.F. Ponce	8	R. Scurbecq	16
J.A. Cáceres	3	Gabi Koschny	30	Eva Redondo	15	V. Soldevila	30
Ó. Cervera	41	Mark Kidger	38	Ina Rendtel	298	D. Spötter	38
J.V. Díaz	31	Detlef Koschny	115	J. Rendtel	521	M. Suárez	15
Roland Egger	2	Ralf Koschack	591	F. Reyes	54	J.M. Trigo	178
R. Fernández	2	Antonio Marín	26	P. Roggemans	258	D. Verde	6

Although it may seem that the number of meteors is large enough, one must remember that very few Taurids are present in the sample. The reason is twofold. Firstly, most meteors were recorded during the Orionid and Leonid campaigns, thus increasing the proportion of members from these showers. Secondly, a large amount of sporadic meteors is required to define the background, so they have to be included as well.

¿From Table 1 it is clear that many more observations are needed for most of the periods, except for those corresponding to the second half of October. This year, the Moon offers the possibility to cover the intervals September 01–04, September 28–October 13, October 27–November 11, and November 26–30, where more data are urgently needed.

Observers should follow the guidelines given in [3], taking special care to estimate the angular velocity of the meteors in degrees per second. An easy method to do this was described in [4]. The center of the field of view should be located no more than 20° from the radiants of the Northern and Southern Taurids. All possible shower members should be plotted, together with those sporadics intersecting the area under study. For this purpose, the *Atlas Brno* is strongly recommended. Your report must include a copy of the maps and the relevant data for each meteor. Do not forget to mention in all cases the subjective accuracy of the plot (1, accurate plot; 2, normal plot; 3, inaccurate plot).

Preliminary results for the Taurids in the period September 16–21 indicate that only one large radiant area is clearly defined, covering both the Northern and Southern Taurid radiants. Because of this, plots of meteors very near the theoretical positions of the Northern and Southern Taurid showers will be needed in order to distinguish the individual radiants.

Old data are, of course, welcome. We will appreciate your contribution if you send us your Taurid plots from 1988 onwards. In fact, most of the already available meteors were collected from 1988. In order to present the analysis as soon as possible, we ask you to mail your observations by the end of December to the following address: *Luis R. Bellot, Instituto de Astrofisica de Canarias, E-38200 La Laguna, Tenerife, Spain.*

Acknowledgments

I thank Jürgen Rendtel and René Scurbecq for sending their data so quickly. I also thank Detlef Koschny for making available the *PosDat* files with meteor plots in the period September–November.

References

[1] R. Arlt, R. Koschack, J. Rendtel, "Results of the IMO Aquarid Project", *WGN* 20:3, June 1992, pp. 114–135.

[2] J. Štohl, V. Porubčan, "Dynamical Aspects of the Taurid Meteor Complex", in *Chaos, Resonance, and Collective Dynamical Phenomena in the Solar System*, S. Ferraz-Mello (Ed.), IAU Symposium 152, 1992, pp. 315–324.

[3] R. Koschack, J. Rendtel, "IMO Aquarid Project", *WGN* 17:3, June 1989, pp. 90–92.

[4] R. Koschack, "Estimating a Meteor's Angular Velocity", *WGN* 18:4, August 1990, pp. 103–104.

Visual Observers' Notes: September–October 1994

Jeff Wood

1. Introduction

Following the excellent activity of the previous two months, observers tend to feel let down when rates return to normal during September and October. Because of this, nowhere near as much observational work has been carried out during this time even though there is much to see.

Table 1 gives a list of the active showers that occur in these months and Table 2 shows the observing conditions moon-wise. The illuminated part of the Moon is always given for 0^h UT on the date indicated. The dates of the phases of the Moon are also given in UT.

For more details, we refer to the *IMO 1994 Meteor Shower Calendar*. Here we highlight some of the showers visible during September and October.

Table 1 – A list of meteor showers to be seen during September and October 1994.

Shower	Activity	Maximum		Radiant			Drift		V_∞	r	ZHR
		Date	$\lambda_\odot$	α	δ	Diam.	$\Delta\alpha$	$\Delta\delta$			
π-Eridanids	Aug 20–Sep 05	Aug 29	155°.7	52°	−15°	6°	+0°.8	+0°.2	59	2.8	
α-Aurigids	Aug 24–Sep 05	Sep 01	158°.6	84°	+42°	5°	+1°.1	0°.0	66	2.5	15
δ-Aurigids	Sep 05–Oct 10	Sep 10	166°.7	60°	+47°	5°	+1°.0	+0°.1	64	3.0	7
Piscids S	Aug 15–Oct 14	Sep 21	177°.7	8°	00°	8°	+0°.9	+0°.2	26	3.0	3
κ-Aquarids	Sep 08–Sep 30	Sep 22	178°.7	339°	−02°	5°	+1°.0	+0°.2	16	3.0	3
Capricornids (Oct)	Sep 20–Oct 14	Oct 03	189°.7	303°	−10°	5°	+0°.8	+0°.2	15	2.8	3
σ-Orionids	Sep 10–Oct 26	Oct 05	191°.7	86°	−03°	5°	+1°.2	0°.0	65	3.0	3
Draconids	Oct 06–Oct 10	Oct 10	197°.0	262°	+54°	5°			20	2.6	
ϵ-Geminids	Oct 14–Oct 27	Oct 20	296°.7	104°	+27°	5°	+1°.0	0°.0	71	3.0	5
Orionids	Oct 02–Nov 07	Oct 21	208°.4	95°	+16°	10°	+1°.2	+0°.1	66	2.9	25
Taurids S	Sep 15–Nov 26	Nov 03	220°.7	51°	+13°	10°/5°	Table 6		27	2.3	10
Taurids N	Sep 13–Dec 01	Nov 13	230°.7	59°	+23°	10°/5°	Table 6		29	2.3	8
Puppid/Velids	Oct 15–Jan 22	several		120°	−45°	20°/5°			40	2.9	

Short Note: 1995 Quadrantid Observations in Puimichel

Paul Roggemans

People interested in observing the 1995 Quadrantids in Puimichel, Southern France, from December 25, 1994, until January 5, 1995, are invited to contact Paul Roggemans. If a group of at least 15 persons can be formed, the price per person and per day (full board) will be 200 FRF. Jürgen and Ina Rendtel have already confirmed their participation. If you are interested, contact me in September or October, but the sooner the better.

Table 2 – Moonlight and observing conditions in September–October 1994.

Date	k	Date	k
Friday September 2	0.17–	Friday October 7	0.05+
Friday September 9	0.14+	Friday October 14	0.73+
Friday September 16	0.85+	Friday October 21	0.98–
Friday September 23	0.91–	Friday October 28	0.47–
Friday September 30	0.31–	Friday November 4	0.00+

New Moon:	September 5, October 5, November 3
First Quarter:	September 12, October 11, November 10
Full Moon:	September 19, October 19, November 18
Last Quarter:	August 29, September 28, October 27

2. Southern Piscids

This weak ecliptic stream is active from August 15 through to October 14. Rates are generally one or two meteors per hour, but on occasions have passed 5 per hour around the maximum which occurs on September 21. With a Full Moon occurring on September 19, the Piscids can best be observed under dark sky conditions from the southern hemisphere during the periods September 1–15 and September 27–October 14. Observers should face the radiant area and plot all Southern Piscids seen taking care to distinguish them from the sporadic background. In particular, the angular velocity must be taken into account.

Table 3 – Radiant positions of the Southern Piscids.

Date	α	δ	Date	α	δ
Sep 15	0°	−02°	Sep 30	13°	+01°
Sep 20	4°	−01°	Oct 05	17°	+02°
Sep 25	9°	00°	Oct 15	26°	+04°

3. κ-Aquarids

This minor ecliptical stream has an activity period from September 8 to 30. It reaches a maximum ZHR of 3 on September 22. Since its period of activity and its radiant position is similar to that of the Southern Piscids, both showers can be observed simultaneously. In 1994, the Full Moon on September 19 means that the κ-Aquarids can be observed under dark sky conditions from September 8 to 14. Southern-hemisphere observers should make their center of field of view somewhere around $\alpha = 345°$ to $0°$ and $\delta = -20°$ to $+20°$. All possible shower meteors should be plotted. Shower association should be carried out very carefully taking note of direction of travel, path length and appropriate angular velocity.

4. δ-Aurigids

As the observing circumstances for the Southern Piscids and the κ-Aquarids are rather unfavorable this year, we do not encourage northern hemisphere observers to watch these showers. They will be much more successful with the δ-Aurigids.

Indeed, the radiant of this minor shower is well situated for observers in the northern hemisphere. The fast ($V_\infty = 64$ km/s) Perseid-like meteors are very striking and the ZHR reaches values of about 7 around September 10. But after more-or-less successful Perseid campaigns, most observers rest on their laurels at that time. That is why our knowledge of this shower is rather poor. With New Moon on September 5, the conditions to monitor its activity are very favorable in 1994. Observers in the northern hemisphere are called upon to pay special attention to this shower in their September observations. Except for the first two hours after dusk, the radiant is sufficiently high in the sky for useful observations with the best conditions in the morning when the radiant approaches the zenith of mid-northern latitudes. Therefore, the morning hours should be preferred for observations. Choose the center of your field of view at about 20° to 30° from the radiant.

All possible δ-Aurigids should be plotted. For final shower association to be carried out at the desk, take into account all criteria (direction and length of the path, and angular velocity). Table 4 shows the position of the δ-Aurigid radiant throughout its activity period.

Table 4 – Radiant positions of the δ-Aurigids.

Date	α	δ	Date	α	δ
Sep 01	51°	+46°	Sep 20	70°	+48°
Sep 10	60°	+47°			

5. October Capricornids

The October Capricornids were discovered in 1972 and provide variable activity from year to year. They are active from September 20 through to October 14 with an overall maximum on October 3. With a New Moon on October 5, the maximum period of their activity will have dark skies. Intending observers should ensure that they face the radiant position and plot all possible shower meteors. Care should be taken in identifying these meteors.

6. Comet Findlay radiant

Observations during September and October have indicated that there is some evidence of meteor activity from the area of the predicted Comet Findlay radiant. Although there will be some interference from the Moon during mid-October, southern-hemisphere observers are requested to make observations of the Comet Findlay radiant a priority in 1994. Since they can be observed simultaneously with the October Capricornids, southern observers should endeavor to monitor both. To do this, they should have a center of field of view situated around $\alpha = 285°$ and $\delta = -20°$, which is midway between the shower radiants. The Comet Findlay radiant should be monitored from September 25 through to October 15. The radiant area is from $\alpha = 260°$ to $280°$ and $\delta = -30°$ to $-42°$. All possible shower members should be plotted and great care should be taken in identifying any meteors coming from the radiant area as such.

7. σ-Orionids

This shower is active from September 10 through to October 26. Its maximum ZHR of 3 meteors per hour occurs on October 5 which means that the Moon does not interfere with the strongest period of activity in 1994. The σ-Orionids have their radiant in the Belt of Orion and so after maximum great care needs to be taken to distinguish them from the October Orionids. This year, the *IMO* is particularly interested in the σ-Orionid activity profile for the period September 29 to October 16 when the skies should be moon-free. Observers in both hemispheres should watch during the last few hours before sunrise and have a center of field situated no more than 30° west or northwest of the radiant. All possible shower members should be plotted and care taken in identifying them.

Table 5 – Radiant positions of the σ-Orionids.

Date	α	δ	Date	α	δ
Sep 15	71°	−03°	Oct 15	93°	−03°
Sep 25	79°	−03°	Oct 25	101°	−03°
Oct 05	86°	−03°			

8. Draconids

The October Draconids reach a sharp maximum on October 10. In 1994, moon-free skies make this period shower a must for monitoring. The Draconids can only be seen from the northern hemisphere and provide extremely variable rates from the ZHR 0 to storm proportions. Situated at a radiant of $\alpha = 262°$ and $\delta = +54°$, the Draconids should be monitored from October 7 to 11 to see if there are any unusual outbursts of activity (probably unlikely) and to determine the structure of the stream. Intending observers should plot all stream members seen unless the ZHR rises above 10 when classified counts may be taken. They should have their center of field of view located no more than 40° from the radiant position. The diameter of the Draconid radiant is 5°. The geocentric velocity of the Draconids equals $V_\infty = 20$ km/s.

9. Orionids

This major shower will have unfavorable Moon conditions in 1994 with the Full Moon occurring on October 19. This is even the more unfortunate, since, in 1993 the Orionids gave an unexpected pre-maximum outburst on October 18 with ZHR values reaching 30 meteors per hour—a very unusual figure that early in the Orionids' activity period.

The Orionids have a complex radiant structure with the center of activity being located just north of the star Betelgeuse at maximum. The Orionids are associated with Comet Halley and, like the η-Aquarids, display a plateau-like maximum. This can vary from year to year but is generally from October 20 to 25. The Orionid maximum occurs on October 21 with a ZHR that is usually in the range of 20 to 30 meteors per hour. Orionids are best observed during the latter part of the night when the radiant altitude rises above 20°. They are observable in both hemispheres and all possible Orionid meteors should be plotted unless the ZHR exceeds 10. Thereafter, classified counts may be taken.

10. Taurids

This shower is broken up into several substreams, the most important of which are called the Northern and the Southern Taurids respectively. The Taurids have one of the longest periods of activity known and last from September 13 through to December 1. They reach a broad maximum in late October and early November. The maxima of November 3 (Southern Taurids) and November 13 (Northern Taurids) given in the radiant list were derived from radio meteor and photographic meteor orbital elements and not visual observations. The last give an uncertain picture. At maximum, Taurid activity is often very erratic with rates ranging from 1–2 meteors per hour to as high as 10 or 15 meteors per hour.

In September and October, the Taurids are best observed during the middle and latter parts of the night. They are noted for their many bright meteors. These are frequently yellow and orange in color, but all of the other colors are also well represented. This together with their relatively low geocentric velocity means that they can be recorded more easily on film than most other showers. Perhaps you could try and photograph some for the *IMO Photographic Meteor Database*.

Since they have a great longevity of activity, the Taurids have parts of their activity period moon-free and others greatly affected by the Moon. They can be easily seen from both hemispheres. When observing the Taurids, all possible shower members should be plotted. In order to distinguish meteors from the branches, the center of field of view should be located between 20° and 40° east or west of the radiant at the same declination.

In September the most favorable center of field of view is around $\alpha = 0°$ and $\delta = +10°$ to $+15°$. This way, κ-Aquarid, Southern Piscid, Northern Taurid and Southern Taurid radiants can all be observed simultaneously. In October the most favorable field of view is located at $\alpha = 80°$ and $\delta = +20°$ which enables both the Taurid radiants together with the Orionid, σ-Orionid and the ε-Geminid radiant to be monitored at the same time. The *IMO* is particularly looking to obtain Taurid ZHR profiles and to investigate the population index during the 1994 Taurid watch.

Table 6 – Radiant positions of the Taurids.

	Taurids North		Taurids South	
Date	α	δ	α	δ
Sep 20	12°	+07°	15°	+02°
Sep 30	21°	+11°	23°	+05°
Oct 10	29°	+14°	31°	+08°
Oct 20	38°	+17°	39°	+11°
Oct 30	47°	+20°	47°	+13°

Call for Observations

Duncan Steel, Anglo-Australian Observatory

The Clementine satellite was a US satellite sent to map the Moon in unprecedented detail, carrying out a successful mission after its launch on January 25, 1994. Its launch booster carried a meteoroid and dust-impact detector, which functioned well until May 10th when it re-entered the atmosphere, recording about 80 impacts in the previous months. During the latter part of that mission, starting on April 29 and continuing for about six orbits, the impact rate rose noticeably. These impacts were apparently due to interplanetary particles and not man-made space debris. Do any meteor observers have records of enhanced activity around the end of April?

[1] W. Kinard, NASA-Langley Research Center, Hampton, Virginia, USA, *Space Flight Environment* 5:3, July–August 1994, p. 6.

Theoretical Radiants of Minor Planets and Comets

Dirk Artoos

Below is a list of theoretical radiants of minor planets and comets, some of which may cause meteor activity during September and October. The list is based on the 1994 *Ephemerides of Minor Planets* and Marsden's 1992 *Catalogue of Cometary Orbits*.

Table 1 - Theoretical Radiants of Asteroids and Comets in September–October 1994.

Name	$\lambda_\odot$	Date	α	δ	V_∞	Distance
P/1911 II (Kiess)	159°.28	Sep 01	91°.3	+39°.3	67.2 km/s	0.00820 AU
P/1698	159°.9	Sep 02	47°.7	+23°.7	70.3 km/s	0.18926 AU
P/1558	160°.24	Sep 02	32°.66	−09°.7	56.6 km/s	0.05085 AU
P/1864 II (Tempel)	160°.88	Sep 03	58°.3	+21°.3	72.0 km/s	0.02920 AU
1986 PA (4034)	163°.97	Sep 06	348°.4	+18°.0	18.5 km/s	0.02154 AU
P/1989 X	164°.6	Sep 07	359°.0	−19°.4	33.0 km/s	0.19442 AU
1989 AZ (5762)	164°.76	Sep 07	351°.4	−37°.8	17.0 km/s	0.16854 AU
P/1847 V	165°.8	Sep 08	359°.56	−19°.2	33.0 km/s	0.19635 AU
P/1932 V	166°.36	Sep 09	60°.34	−39°.9	43.0 km/s	0.15150 AU
P/1264	168°.845	Sep 11	231°.9	+22°.3	23.8 km/s	0.11298 AU
P/1906 V (Finlay)	168°.92	Sep 11	296°.3	−32°.4	15.6 km/s	0.04873 AU
P/1907 IV (Daniel)	169°.36	Sep 12	347°.1	+04°.3	31.7 km/s	0.06749 AU
P/1854 III	169°.48	Sep 12	54°.4	−15°.2	58.2 km/s	0.01850 AU
1986 LA (3988)	170°.06	Sep 12	214°.6	+42°.7	13.5 km/s	0.19696 AU
Hephaistos (2212)	171°.8	Sep 15	157°.0	−00°.9	31.0 km/s	0.12466 AU
P/1788 II	174°.28	Sep 17	60°	−50°	44.6 km/s	0.19228 AU
P/1893 II	175°.13	Sep 18	65°.3	+10°.9	70.3 km/s	0.11462 AU
Midas (1981)	175°.4	Sep 18	140°	+29°.9	10.6 km/s	0.03669 AU
Bacchus (2063)	176°.66	Sep 19	7°.3	−24°	16.2 km/s	0.10531 AU
P/1683	178°.63	Sep 21	144°.1	+50°.18	53.5 km/s	0.11085 AU
P/1763	179°.5	Sep 22	45°.2	−23°.2	47.6 km/s	0.01956 AU
P/1790 I	181°.53	Sep 24	115°.8	+38°.13	67.5 km/s	0.03532 AU
P/1977 XIV (Kohler)	182°.45	Sep 25	239°.7	+67°.7	33.7 km/s	0.01124 AU
P/1766 II	182°.00	Sep 25	177°.0	+09°.1	30.5 km/s	0.13186 AU
P/1769	185°.61	Sep 28	24°.6	+23°.4	45.7 km/s	0.11257 AU
1988 TA (5704)	186°.17	Sep 29	199°.5	−01°.0	16.7 km/s	0.00658 AU
1994 EK	186°.56	Sep 29	359°.7	−13°.8	19.0 km/s	0.05464 AU
P/1961 II (Candy)	186°.998	Sep 30	110°.7	+38°.2	67.0 km/s	0.18052 AU
Cuyo (1917)	190°.26	Oct 03	291°.5	+57°.47	18.4 km/s	0.07565 AU
1994 ES_1	192°.26	Oct 05	186°.5	−04°.8	21.4 km/s	0.00651 AU
1994 CK_1	194°.53	Oct 07	307°.6	−32°.2	13.3 km/s	0.03552 AU
P/1987 III	195°.24	Oct 07	94°.0	+27°.7	72.0 km/s	0.04758 AU
P/1987 III	195°.26	Oct 08	94°.0	+27°.7	72.0 km/s	0.04760 AU
P/1825 II	195°.4	Oct 08	138°	+77°	55 km/s	0.11601 AU
Rha Shalom (2100)	197°.03	Oct 10	50°.7	+48°.0	17.0 km/s	0.14882 AU
P/1939 IX (Friend)	197°.31	Oct 10	160°	+58°	51.6 km/s	0.16142 AU
P/1757	198°.42	Oct 11	22°.28	+18°.0	37.0 km/s	0.07572 AU
P/568	198°.47	Oct 11	226°.2	−26°.54	21.0 km/s	0.06789 AU
P/1723	198°.95	Oct 12	115°.3	−07°.5	65.0 km/s	0.06048 AU
1994 CN_2	200°.77	Oct 14	236°.0	−26°.7	13.3 km/s	0.02453 AU
P/1957 IX	201°.2	Oct 14	83°.7	+33°.8	66.0 km/s	0.07772 AU
P/1864 IV (Baeker)	204°.1	Oct 17	212°.0	+43°.1	36.4 km/s	0.03449 AU
P/-86 (Halley)	205°.5	Oct 19	91°.6	+15°.6	67.0 km/s	0.04672 AU
P/1779	206°.85	Oct 20	39°	−28°	31.5 km/s	0.01832 AU
1993 TZ	207°.16	Oct 20	256°.0	+11°.7	16.4 km/s	0.00450 AU
P/1580	207°.4	Oct 20	65°.7	−19°.6	43.3 km/s	0.12644 AU
Hathor (2340)	208°.26	Oct 21	186°.4	+09°.5	17.0 km/s	0.00623 AU
P/1964 VIII (Ikeya)	210°.9	Oct 24	107°.8	+26°.8	70.0 km/s	0.12221 AU
P/1986 III (Halley)	211°.3	Oct 24	97°.2	+15°.0	66.5 km/s	0.15369 AU
1993 VD	211°.41	Oct 25	187°.2	−06°.6	19.0 km/s	0.01540 AU
P/1988 V (Liller)	212°.2	Oct 25	81°.7	−29°.0	45.0 km/s	0.08023 AU
1944 CC	213°.6	Oct 27	203°.8	−20°.0	25.0 km/s	0.11742 AU

Photographic Observers' Notes: September-October 1994

Jürgen Rendtel

In the June issue's Photographic Notes, we already pointed out that even single-station meteor photographs may help to solve some questions [1]. One of such questions regards the activity and precise radiant of the δ-Aurigid meteor shower. The indications from visual (plotting) data and meteoroid orbits determined from double-station photographs are strong enough to prove the existence of this shower [2].

There are hints on two possible activity periods centered around September 10 and October 8. The visual data and the orbits seem to prove that this is one shower. Photographic trails may help to follow the radiant during the entire suspected period. For this purpose, we need photographs of meteors possibly belonging to this shower. The geocentric velocity of the shower members is high (64 km/s). Consequently, the angular velocities will be large for shower meteors at large distance from the radiant and close to the zenith. Therefore we recommend to use fast lenses (e.g., $f/1.4$, $f = 50$ mm), fast black-and-white film (at least ISO 400/27°) and a field centered some 40° west or east of the radiant at about the elevation of the radiant. In order to achieve a good distribution around the radiant, we may choose fields both west (before 1^h local time) and east (after 1^h local time) of the radiant in the course of the night.

Please, send your successful photographs (also of other than these meteors) to Jürgen Rendtel (address on inside back cover) for analyses and inclusion in the *PMDB* of the *IMO*.

[1] J. Rendtel, "Photographic and Video Observations During the Perseid Peaks", *WGN* 22:3, June 1994, pp. 90–92.

[2] J. Rendtel, "Radiants and Orbits of δ-Aurigids and September Perseids", *Proc. IMC 1992*, 1992, pp. 67–72.

Telescopic Observers' Notes: September–October1994

Malcolm J. Currie

The most regular contributor of late continues to be Chris Hall of Stoke, UK. In May and June he secured 46 meteors in 4.45 hours during four nights curtailed by summer twilight. I myself have been making observations when the weather and skies permit. However, the Perseid campaign was thwarted by cloud. It was only sufficiently clear on parts of four nights, August 8-9, and 12-13 to 14-15, netting over 100 meteors. There was no abnormal telescopic-Perseid activity. Reports for August 10–13 would be particularly relevant, and I urge observers to submit their Perseid reports soon.

Forthcoming events

According to magazines and popular books, the "summer" showers are over and since there is no major shower until the Orionids, there's nothing to do for a couple of months. This is *wrong*! Unfortunately, many observers seem to believe them. This is a great shame as September is one of the best months for telescopic meteors in terms of numbers, piquant minor showers, and opportunities to discover radiants. The last of these arises simply because September has been neglected so much in the past.

The most gripping area to cover lies in Auriga-Perseus-Cassiopeia. There are several high-inclination streams present that produce swift-moving ($V_\infty \approx 65$ km/s) meteors. At least one is believed to have sub-streams present; according to Gary Kronk's [1] analysis from radio and photographic data the *δ-Aurigid* shower has at least four filaments. These are most prominent during early October. Another component (formerly called the September Perseids [2]) peaks around September 10 radiating from around $\alpha = 55°$ and $\delta = +46°$. Both of these peaks are well placed in 1994. In October, the main two components are only separated by about 5°, which is difficult to resolve visually, but should be possible telescopically. The shower persists from early September through to mid-October. Precise activity dates await determination from your observations.

Jürgen Rendtel [2] also commented that the δ-Aurigid shower has a similar orbit to the sungrazing Kreutz-group comets. These have orbits believed to be in the end state of evolution, and hence give weak activity near or below the visual detection threshold. He speculates that there may be more of these highly inclined meteor showers awaiting discovery. In my opinion, telescopic and video techniques stand the best chance of finding them. Indeed, telescopic observations may have already detected some. A strong radiant at $\alpha = 43°$ and $\delta = +49°$ and another possible one 13° further west were found during mid-September 1991. Also during the first half of September, there are the *β-Cassiopeids* comprising very faint and swift meteors from a compact radiant. [3] Since I first noted this shower in 1988, we have seen few likely members. This may be due to some periodic behaviour, though this is improbable if the stream is old. More likely is the faintness and speed of the meteors that makes them hard to detect with small binoculars and/or under bright sky conditions.

Better known from this portion of sky are the *α-Aurigids*. This year, a waning crescent moon will interfere and only from the maximum (September 1) will observations be worthwhile. It is known to have occasional visual outbursts a few times the normal peak rate, and undoubtedly many have been missed. What we do not know is their frequency, and whether or not an outburst is more or less visible at telescopic magnitudes. Thus this shower is well worth monitoring.

So to summarize, we have a complex of radiants during September and October whose telescopic-activity dates and radiant parameters are at best poorly determined and at worst unknown. They give peak telescopic rates up to the sporadic background, though most of the time activity is a few times weaker than that. Observations by all methods are badly needed over a number of years to describe the properties of these showers, and to investigate if any are interrelated. Thus, this year I urge northern telescopic observers to investigate this region during September 1–15 and September 30–October 14. Concentrate on accurate plotting and careful speed estimation, using at least three field centers per night to reduce radiant occlusions and to give weight to any possible-radiant identifications. Since the radiants have a low elevation during the evenings, watches after midnight local time are particularly valuable. In September, you can follow several radiants simultaneously given a judicious choice of fields. I recommend charts 36 and 49, and/or 17 and 50 for the *β*-Cassiopeids which should be prime target until about 23^h. For the remainder of the night use charts 36, 37, 51, 75, 76, and 39 for the radiants in Perseus and Auriga. The last two are best for the *α*-Aurigids. As a bonus, these fields should let us ascertain whether or not there is a shower from $\alpha = 122°$ and $\delta = +39°$ at $\lambda_\odot = 192°$, as suspected from observations made in 1989. For October's *δ*-Aurigids, I should select charts 19, 53, 54, 56, and 57. Chart 53 is somewhat distant from some of the sub-radiants. The alternative is 39, which is good for discriminating filaments A–C, but its center lies close to radiant D.

During the evenings of October 7–11, it is always worth spending an hour or two checking the enigmatic *Draconids*. This shower is capable of storm activity, yet often has disappointed when high rates have been predicted. Usually, activity is low or non-existent. This does not mean that this shower is only worthy of our attention when the parent comet P/Giacobini-Zinner is near perihelion and high rates are possible. The Draconid shower is young and we have an opportunity to watch its development into a mature stream. If the models of stream evolution are correct, we would expect a gradual dispersal of the meteoroids around the stream orbit. This can be detected via monitoring each year. The smallest particles disperse quickest due to the Poynting-Robertson and Yarkovsky-Radzievskii effects, and since the Draconids are rich in faint meteors, it is especially important to make telescopic watches to look for activity. I recommend charts 70 and 86.

For those further south, there are the fast *σ-Orionids*. This weak, long-duration shower is rich in faint meteors, and is well placed in 1994, with the maximum occurring a day before New Moon. Little is known about it, so a series of post-midnight watches during early October should reveal unknown aspects, such as its radiant properties. The suggested charts are 141 and 143, with 142 if time permits.

The *Orionids* are badly affected by moonlight. Observations may be possible at the extremes of the shower before October 15 and at the end of the month. The *Taurids* being a long-duration shower can always be observed during some part of its activity. Renown for moderately bright meteors, if not fireballs [4], this shower and other members of the Encke complex are not obvious targets for the telescopic observer. However, we can provide provide useful radiant data, separating the two main components. The low angular speed coupled with the long paths increases the probability of detection.

References

[1] G.W. Kronk, "Meteor Showers: A Descriptive Catalogue", Enslow, 1988, pp. 185–188.

[2] J. Rendtel, "Radiants and Orbits of Delta Aurigids and September Perseids", in *Proceeding 1992 IMC*, 1992, pp. 67–73.

[3] M.J. Currie, *BAA Meteor Section Newsletter, Telescopic Appendix*, October 1988, pp. 3–4.

[4] N.M. Bone, "Visual Observations of the Taurid Meteor Shower, 1981–1988", *J. Brit. astr. Assoc.* 101:3, 1991, pp. 145–152.

Call to our North-American readers:

As last year the European observers, many North-American meteor observers may have made fine Perseid photographs during the recent outburst, about which you can read more on the next page. If you think your photograph is of reproducable quality, please send a print to WGN *so that we can publish it, ... may be even on the front cover!* (Editor)

North-American Observers Witnessed 1994 Perseid Outburst

compiled by Peter Brown and Marc Gyssens

Perseid ZHR's were normal from August 11.88 UT till August 12.30 UT being in the range of about 50–100. Starting at August 12.35, the ZHR began climbing significantly and reached a peak near 250 in the half hour interval centred about August 12.45 UT. The results from the single group at Honey Lake, California, reporting detailed quantitative data are supported by qualitative data from more casual observers on the West coast. The ZHR dropped back to normal levels of about 50–100 by August 12.50 UT. No results immediately after August 12.50 UT are yet avaliable. The shower had returned to normal activity levels by August 12.88 based on European data from Austria and the UK. Radio results support a peak near August 12.45 with higher rates from August 12.35 till August 12.47.

A chief source of information are the observations by J. Rendtel, I. Rendtel, A. Knöfel, and D. Holman from Honey Lake, California, under excellent sky conditions (limiting magnitude better than +6.5. They have reported the following details concerning their observation of the outburst near August 12.45 UT (solar longitude $\lambda_\odot = 139°.58$, eq. 2000.0).

Table 1 – Average ZHRs derived from the observations from Honey Lake, California.

Date (UT)	ZHR	Date (UT)	ZHR	Date (UT)	ZHR
Aug 12.21	50	Aug 12.33	70	Aug 12.45	225
Aug 12.25	60	Aug 12.38	110	Aug 12.48	150
Aug 12.29	60	Aug 12.42	180	Aug 12.50	80

The observers suggest that the outburst started near August 12.35 UT (8^h30^m UT) and was over by August 12.5 (12^h00^m UT). The peak time is August 12.45 (10^h30^m–11^h00^m UT), and the peak ZHR (derived from the 15-minute interval 10^h45^m–11^h00^m) is 225. However, shorter intervals (of about 5 minutes) between 10^h30^m and 11^h00^m UT easily lead to equivalent ZHRs near 400–500. Several fireballs were observed during the outburst.

The above findings are confirmed by several other observers.

First, there are a number of qualitative reports from not necessarily experienced observers we wish to mention. T. Wright (Marin County, California) reports intense activity from 10^h00^m–11^h00^m. D. Chamberlin (Mt. Hood, Oregon) saw a strong maximum at 10^h45^m UT, with a visual rate of 3–4 meteors per minute. G. Elmore (Santa Rosa, California) mentions that a group of three, observing different sections of the sky, recorded a peak rate of 39 meteors per minute near 10^h45^m UT, which tapered to 5 per minute for the group of 3 observers by 11^h00^m UT. He compared the display to what he had seen visually during the 1966 Leonids. J. Paulson (Mary's Peak, Oregon) estimated a peak rate of 3–4 meteors per minute in the interval 10^h45^m–11^h30^m UT. C. Tribolet (Morgan Hill, California) reports peak rate higher than seen last year in California. M. Smithwick (San Francisco, California) qualitatively estimates between 80–100 meteors between 10^h30^m-11^h30^m UT under urban skies. B. Templeton (Freemont Peak State Park, California) reports group observations suggesting peak period of activity from 10^h30^m to 11^h30^m UT, with several minutes of activity where a meteor was visible every 2–3 seconds. R. Royer (Bishop, California) observed in a group of 11. He reports that rates began picking up after 9^h00^m UT and peaked between roughly 11^h00^m and 11^h30^m UT. Many fireballs were observed up to magnitude −9. P. Strosser (Sierra Nevada Mountains, California) recorded a strong outburst observed under excellent sky conditions, peaking between 9^h and 11^h UT. Numerous fireballs were recorded in this time. P. Jenniskens (California) reports that a peak visual rate of 3 meteors per minute was reached at 11^h10^m UT.

B. Lunsford (Chula Vista, California) reports generally cloudy conditions with only half an hour of clear observing centred about August 12.49 with a ZHR of around 100 under a limiting magnitude of 6.3. Several observers not located near the West Coast noticed Perseid activity rising more strongly than normal towards twilight. Among them were R. Huziak (Saskatoon, Saskatchewan), R. Taibi (McKendry, Virginia), D. Swann (Oklahoma), M. Hann (Mounds, Oklahoma), and T. Dickinson (Yarker, Ontario). Observers near the American East Coast, such as P. Gray (Halifax, Nova Scotia) and N. McLeod III (Ft. Myers, Florida) did not notice significantly enhanced activity. R. Hawkes (Sackville, New Brunswick), running MCP-CCD video intensified system to lm = +8.5 from 1^h15^m–8^h30^m UT, reports no spectacular rates at low magnitudes and rates below 1993 numbers at corresponding times. C. Steyaert (Belgium) reports that M. De Meyere (Deurle, Belgium) recorded relative maximum radio forward scatter rates between 10^h00^m and 11^h00^m UT on August 12 with rates corresponding to 3.5 times similar level of activity the previous night. There was a broad maximum in rates between 8^h00^m and 12^h00^m UT. S. Ennis (Elizabethtown, Kentucky) reports that radio observations on the morning of August 12 at 144 Mhz were generally poor. Most intense flurries of activity were heard between 10^h48^m and 11^h18^m UT.

While this is being compiled, few reports are available from the period shortly before and after the outburst. Many European observers seem to have had clouded skies. From what is available now (mostly Hungarian reports), it seems that nothing unusual happened during the European nights of August 11-12 and 12-13.

Progress in Meteor Science

Articles in this section have been formally refereed by at least one professional and one experienced, knowledgeable amateur meteor worker, and deal with global analyses of meteor data, methods for meteor observing and data reduction, observations with professional equipment, or theoretical studies.

Spatial Number Densities and Errors from Photographic Meteor Observations under Very High Activity

Luis Ramón Bellot Rubio

A procedure to compute meteoroid spatial number densities and flux densities from photographs is presented. It follows from the visual method of Koschack and Rendtel with slight changes. Some parameters are recomputed and hints are given on how to produce useful photographic observations. Finally, an analysis of the expected errors is performed. It turns out that the systematic error caused by the uncertainty in the exponent of the radiant zenithal distance correction has important effects on the accuracy of the flux density. Therefore, a detailed investigation of this topic is suggested.

1. Introduction

The recent possibility of enhanced Perseid activity in 1993–1994 and the expected return of the Leonid storm in 1998–1999 have led to a growing interest in the computation of spatial number densities from photographic observations.

Under very high activity, visual observations become more and more inaccurate because of the change in the perception coefficients and the reduction of the available time to note down the data for each meteor. The great advantage of the visual technique (i.e., the possibility of recording meteors down to magnitude +5 or +6) does not hold any longer since the observer cannot keep up with the activity. As a consequence, one has to restrict the count to meteors brighter than a certain magnitude threshold. The "effective" limiting magnitude for visual observations under storm conditions thus becomes comparable to that of photography, which allows us to benefit from the objectivity of the photographic method.

Photography offers a number of advantages. It is possible, for instance, to compute with great precision the area surveyed by the camera field at a given meteor level. Moreover, it may be assumed that the perception coefficients of the camera are constant and even equal to unity if we take into account the meteor limiting magnitude. The photographic technique has also some disadvantages, however. The most important of them are the restricted field of view (which in turn means that less meteors are recorded) and the impossibility of obtaining actual meteor magnitudes. The reason is that the geocentric velocities of some showers (Perseids, Leonids) are near the upper limit of 72 km/s and produce a high percentage of trained meteors [1,2] As the photograph does not separate the light of the meteor itself from the train light, there is a pollution that varies the photographic magnitude of the meteor. However, such an effect may be of secondary importance when calculating the population index, since the meteors just have to be grouped in intervals of one magnitude width and we may assume that a comparable portion of meteors in consecutive magnitude classes show trains [3].

Several parameters are required before spatial number densities, or flux densities, can be computed from photographs. This paper extends the visual method developed by Koschack and

Author's address: Instituto de Astrofísica de Canarias, C/ Vía Láctea s/n, E-38200 La Laguna, Tenerife, Spain, e-mail: lbellot@iac.es.

WGN, the Journal of the International Meteor Organization, Vol. 22, No. 4, August 1994, pp. 118–130.

Rendtel [4] to the photographic case and analyzes in detail the expected error of the calculations.

2. Photographic meteor limiting magnitude and choice of camera field center

Obviously, the larger the number of recorded meteors is, the more accurate the results are. One of the factors that influences the number of recorded meteors is the photographic meteor limiting magnitude, *plm*. This quantity depends on the camera set-up, the film type and, more importantly, on the meteor angular velocity. Two meteors of the same visual magnitude have different photographic magnitudes if their angular velocities are different. The slower the meteor is, the brighter it appears on the photograph. The variation in apparent magnitude, due to a difference of angular velocity, can be described by

$$m_1 = m_2 - 2.5p \log \frac{\omega_2}{\omega_1}, \tag{1}$$

where m_i is the photographic magnitude of the meteor with angular velocity ω_i $(i = 1, 2)$, and p is the Schwarzschild exponent accounting for the failure of the reciprocity law [5,6].

If we want to record as many meteors as possible, we should look for the sky area in which meteors have the slowest angular velocity. The angular velocity of a meteor depends on the altitude h of its starting point above the horizon and on the angular distance ξ from the starting point to the radiant [7]:

$$\omega = \frac{v_\infty}{H} \sin \xi \sin h, \tag{2}$$

where v_∞ is the pre-atmospheric velocity of the meteoroid and H the height of the meteor level.[1] Clearly, the slowest angular velocities are obtained when $\xi \approx 0$, i.e., when the meteor appears close to the radiant. In principle, this area is the best choice to point the camera, since it allows the faintest meteors to be recorded and hence improves *plm*.

One problem of a near-radiant camera field, however, is the identification and photometry of the very short or almost point-like meteor trails occurring there. It also has the great disadvantage of a non-constant photographic limiting magnitude over the field, because the angular speed of the shower meteors does vary strongly near the radiant. Table 1 summarizes the change of *plm* across the field of a standard 35 mm, $f = 50$ mm camera pointed to the radiant as a function of the radiant altitude h_R. The data have been computed using the angular velocity of meteors at $\xi = 5°$ and $\xi = 20°$, and then applying equation (1) with $p = 0.8$. Such enormous differences have to be avoided to determine the number of meteors per magnitude range (which will be used afterwards to obtain the population index of the shower).

Table 1 – Reduction of the photographic limiting magnitude $\Delta plm \equiv plm(\xi = 20°) - plm(\xi = 5°)$ across the field of a 35 mm, $f = 50$ mm camera pointed to the radiant.

h_R	20°	40°	60°	90°
Δplm	+1.55	+1.37	+1.26	+1.14

It should be clear now that the most important criterion is the constancy of *plm* over the photograph, so the next step is to find the area of the sky in which the angular velocity of the shower meteors varies as little as possible. We follow the usual procedure and equate the partial derivatives of ω in (2) to zero, which gives the solution $\xi = 90°$, $h = 90°$ [8]. These requirements cannot be satisfied except when the radiant lies on the horizon and the camera points to the zenith, but it is still possible to minimize the change of angular velocity.

[1] Notice that, if v_∞ is given in km/s and H is given in km, then ω is given in rad/s.

First, the values ξ and h should be as large as the geometry allows. Thereto, the camera must be pointed 180° away from the radiant in azimuth [8], i.e., $a_f = a_R \pm 180°$.[2] If $a_f = a_R \pm 180°$, then the condition $h \approx 180° - \xi - h_R$ holds, reducing the number of variables in equation (2). This reduction simplifies the calculation of h_f, the optimum altitude for the camera center, which turns out to depend on h_R through

$$h_f = 90° - \frac{h_R}{2}. \tag{3}$$

Table 2 lists some numerical values of h_f in terms of the radiant altitude h_R. Since the angular velocity of the shower meteors varies little across the camera fields specified by Table 2, the change of the limiting magnitude due to different velocities is also very small (cfr. the third column of Table 2, where Δplm has been calculated for a 35 mm, $f = 50$ mm camera). Unfortunately, the angular velocity of the shower meteors reaches its maximum in these fields, which reduces the limiting magnitude to a great extent. Table 3 shows the reduction of *plm* with respect to a field centered at the radiant. In order to improve *plm*, high-speed films (e.g., ASA 3200) are strongly recommended. It goes without saying that the importance of a meteor storm deserves the best available film.

Table 2 – Optimum camera field elevation h_f as a function of the radiant elevation h_R. The third column represents the change of the limiting magnitude *plm* across the camera field when the longest edge of the photograph is parallel to the horizon. It has been computed by using the variation of the angular velocity of the shower meteors from the center to the edges of the photograph.

h_R	h_f	Δplm	h_R	h_f	Δplm
20°	80°	0.05	70°	55°	0.07
40°	70°	0.05	80°	50°	0.08
50°	65°	0.06	90°	45°	0.09
60°	60°	0.06			

Table 3 – Reduction of the photographic meteor limiting magnitude, Δplm, for a 35 mm, $f = 50$ mm camera centered at the elevations given in Table 2 with respect to a field pointing to the radiant.

h_R	20°	40°	50°	60°	70°	80°	90°
Δplm	+2.11	+1.65	+1.48	+1.33	+1.20	+1.07	+0.94

We do not know how to compute the photographic meteor limiting magnitude of a given exposure on theoretical grounds. Several equations have been tested and showed a good qualitative (but not quantitative) behavior [9]. The major drawback is that they usually ignore a number of relevant effects such as the presence of trains or the darkness of the sky. Meanwhile, simultaneous visual-photographic observations indicate that the typical photographic limiting magnitude for meteors ranges from roughly +1 to +3, depending on ω and the film speed [9]. These results suggest setting the reference photographic limiting magnitude as +3.5 (remember that the +3 magnitude class includes meteors from +3.5 to +2.5). Apart from being a reasonable value, this choice has a further advantage: it permits the comparison of spatial number densities obtained from photographs and from visual observations under very high activity.

[2] Note that Trigo [9] wrongly sets the optimum azimuth of the camera as 45° away from the radiant azimuth. He obtains this result on the assumption that such a field has the highest probability of meteor appearances, but a little thought reveals that this is not true when the negatives are projected onto the meteor layer from the observer's site.

3. The projected area at the meteor level

Once the optimum camera field center has been defined, the procedure requires to know the area surveyed by the photograph at the meteor level. From now onwards, we assume a camera field of $27\overset{\circ}{.}0 \times 39\overset{\circ}{.}6$, which corresponds to standard film dimensions of 24 mm $\times$ 36 mm in a camera with $f = 50$ mm. These values are obtained from the well-known formula $L = 2\arctan(l/2f)$, where l is the length of the negative in mm, and L the corresponding angular aperture in degrees.

As in [4], the data are reduced to a standard area $A_{\rm red}$ for which there is no extinction ε and the distance to the observer is assumed to be 100 km. If A_i represents the projected geometrical area of a small portion of the photograph at distance d_i from the camera and extinction ε_i, the reduced area $A_{\rm red}$ may be computed from

$$A_{\rm red} = \sum_i A_i \, r^{5 \log \frac{100 \text{ km}}{d_i} - \varepsilon_i}, \tag{4}$$

where the index i is such that all zones of the photograph enter the summation.

The details for the calculation of $A_{\rm red}$ are explained in the Appendix. The numerical procedure assumes that the longest edge of the photograph is parallel to the horizon. Average extinction values from [10] have been used. We must carefully define the height H of the meteor level. Any characteristic height of the meteor trajectory depends on velocity, mass and zenith angle (in decreasing order) [11,12]. If we select the height H_b of the beginning of the photographic trajectory as the height of the meteor layer, H will also depend on *plm*. However, there are two reasons in favor of this choice. First, deriving an accurate relationship between the above mentioned parameters is still impossible due to the lack of data on individual showers. Secondly, the dependence of H_b on mass and zenith angle is much less important than its dependence on velocity (which is not true if we use, for instance, the height of maximum intensity). This way, only one height is required for each shower. The small variations of H that might be present due to the slight dependence of H_b on mass and zenith angle will be reflected in an increase of the standard deviation of H.

The best photographic compilation of heights for different showers is the survey of Jacchia et al. [11]. The limiting magnitude in that survey was about +2.5, close to the photographic limiting magnitude achievable nowadays by standard cameras equipped with high sensitivity films. Since the threshold of detection is similar in both cases, we may use the mean values of H_b reported in [11] as the height H of the meteor layer. It turns out that $H = (100 \pm 9)$ km for all meteors (including sporadics), whilst for Perseids H increases up to (114 ± 3) km. The paper by Jacchia et al. does not contain enough data for Leonids, and thus we use the graphically reduced Super-Schmidt meteors of McCrosky and Posen [13]. Despite the poorer quality of these meteors, the heights given in [13] still constitute a valid approximation, yielding $H = (118 \pm 6)$ km for Leonids.

Figure 1 shows $A_{\rm red}$ when $H = 100$ km. The qualitative behavior of $A_{\rm red}$ as a function of the population index differs from the visual case (cfr. Figure 5 in [4]). The smaller the altitude of the camera field is, the larger the photographic reduced area becomes. The population index does not change this trend, except for very high r-values that never occur in practice. Consequently, we shall obtain more reliable results when the radiant is near the zenith, since the surveyed area will be larger (cameras pointing to smaller elevations).

Tables 4–6 give $A_{\rm red}$ for $45^\circ \leq h_f \leq 90^\circ$ and $H = 100$ km, 114 km, and 128 km, respectively. The error ΔA_i when computing the geometrical areas A_i can be ignored since its contribution to $\Delta A_{\rm red}$ never exceeds 2 km^2. The uncertainty of the extinction values has not been taken into account as it depends on the sky conditions; however, it should be negligible for fields near the zenith. Moreover, small r-values (which are likely to occur during storms) reduce the influence of $\Delta\varepsilon$. The most important error is thus the error σ_H. Accordingly, we expect $\Delta A_{\rm red} \approx 0.08 A_{\rm red}$ for $H = (100 \pm 9)$ km, $\Delta A_{\rm red} \approx 0.025 A_{\rm red}$ for Perseids ($H = (114 \pm 3)$ km), and $\Delta A_{\rm red} \approx 0.06 A_{\rm red}$ for Leonids ($H = (118 \pm 6)$ km).

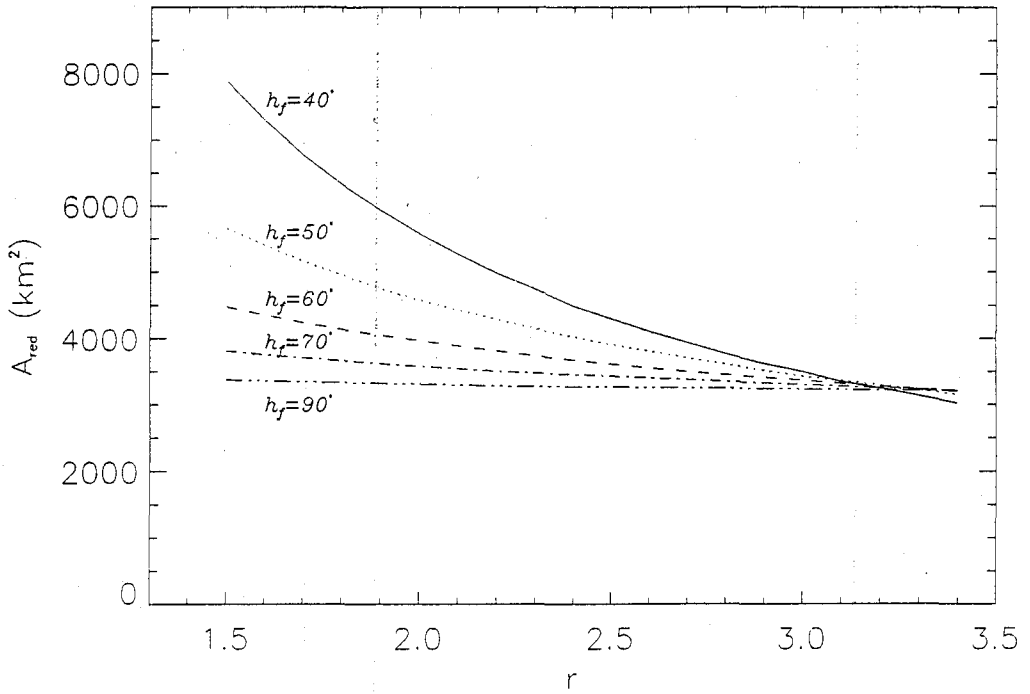

Figure 1 – Reduced areas $A_{\rm red}$ as a function of the population index r and the camera field elevation h_f. The height of meteor appearances is assumed to be H = 100 km.

Table 4 – Reduced areas $A_{\rm red}$ (km^2) as a function of r and the camera field center elevation h_f for $H = 100 \pm 9$ km. The maximum error $\Delta A_{\rm red}$ is 8% of $A_{\rm red}$.

r	h_f								
	45°	50°	55°	60°	65°	70°	75°	80°	90°
1.5	6588	5659	4976	4482	4094	3813	3616	3480	3376
1.6	6199	5404	4793	4359	4016	3760	3581	3457	3363
1.7	5853	5165	4640	4242	3943	3712	3550	3437	3348
1.8	5543	4957	4503	4142	3876	3668	3521	3420	3338
1.9	5279	4757	4375	4055	3813	3628	3496	3404	3327
2.0	5035	4584	4250	3975	3750	3589	3476	3388	3316
2.1	4814	4433	4128	3895	3696	3549	3455	3372	3303
2.2	4590	4293	4026	3820	3647	3512	3434	3354	3280
2.3	4419	4157	3932	3745	3598	3484	3418	3342	3289
2.4	4251	4028	3847	3677	3550	3461	3400	3329	3276
2.5	4098	3911	3759	3618	3502	3434	3380	3316	3270
2.6	3953	3812	3669	3560	3471	3410	3358	3303	3264
2.7	3821	3709	3599	3501	3438	3382	3336	3289	3257
2.8	3694	3616	3527	3455	3404	3354	3316	3277	3251
2.9	3590	3521	3457	3414	3369	3329	3298	3264	3245
3.0	3471	3430	3404	3371	3334	3306	3280	3251	3237
3.1	3368	3368	3351	3324	3305	3284	3260	3239	3230
3.2	3289	3300	3295	3284	3274	3260	3243	3228	3223
3.3	3198	3224	3237	3238	3239	3238	3228	3218	3217
3.4	3103	3156	3182	3200	3214	3219	3213	3210	3210

Table 5 – Reduced areas A_{red} (km^2) as a function of r and h_f for $H = 114 \pm 3$ km (the Perseid case). The maximum error ΔA_{red} is 2.5% of A_{red}.

r	h_f								
	45°	50°	55°	60°	65°	70°	75°	80°	90°
1.5	7455	6412	5647	5073	4649	4329	4107	3957	3843
1.6	6898	6018	5351	4870	4473	4202	4005	3867	3758
1.7	6410	5665	5091	4651	4329	4084	3899	3777	3686
1.8	5987	5347	4871	4475	4195	3969	3806	3697	3617
1.9	5613	5067	4637	4319	4065	3866	3723	3628	3551
2.0	5274	4830	4454	4180	3944	3779	3659	3569	3489
2.1	4975	4577	4284	4031	3842	3690	3569	3486	3441
2.2	4717	4385	4122	3906	3739	3601	3487	3430	3379
2.3	4457	4206	3974	3799	3644	3518	3443	3391	3348
2.4	4244	4025	3846	3679	3552	3462	3402	3333	3277
2.5	4044	3869	3708	3580	3479	3407	3322	3273	3245
2.6	3861	3720	3595	3488	3411	3319	3247	3225	3199
2.7	3691	3586	3486	3409	3323	3251	3209	3180	3156
2.8	3539	3461	3391	3308	3245	3206	3174	3144	3125
2.9	3405	3348	3280	3231	3197	3159	3134	3109	3086
3.0	3262	3223	3201	3172	3137	3112	3093	3061	3046
3.1	3141	3139	3124	3103	3084	3064	3036	3021	3014
3.2	3035	3048	3040	3028	3022	2998	2978	2991	2987
3.3	2908	2938	2953	2964	2964	2954	2952	2958	2954
3.4	2825	2868	2890	2903	2909	2915	2919	2915	2921

Table 6 – Reduced areas A_{red} (km^2) as a function of r and h_f for $H = 118 \pm 6$ km (the Leonid case). The maximum error ΔA_{red} is 6% of A_{red}.

r	h_f								
	45°	50°	55°	60°	65°	70°	75°	80°	90°
1.5	7706	6630	5841	5246	4816	4480	4249	4097	3974
1.6	7094	6187	5508	4997	4620	4321	4116	3975	3870
1.7	6567	5806	5218	4793	4430	4182	4003	3871	3776
1.8	6104	5455	4965	4562	4278	4059	3890	3786	3699
1.9	5707	5154	4735	4390	4137	3931	3784	3683	3613
2.0	5340	4895	4506	4229	4000	3824	3696	3611	3538
2.1	5013	4630	4324	4072	3875	3727	3618	3538	3473
2.2	4749	4411	4153	3930	3771	3628	3511	3445	3394
2.3	4468	4217	3986	3812	3657	3533	3451	3399	3353
2.4	4244	4024	3847	3679	3554	3463	3402	3334	3277
2.5	4033	3860	3696	3571	3474	3395	3306	3264	3242
2.6	3842	3695	3576	3474	3389	3298	3232	3204	3171
2.7	3660	3559	3463	3378	3288	3227	3193	3162	3137
2.8	3496	3430	3347	3268	3222	3182	3146	3116	3089
2.9	3360	3296	3239	3202	3158	3123	3095	3060	3043
3.0	3201	3189	3161	3123	3093	3058	3013	3012	3005
3.1	3097	3089	3064	3037	3013	2985	2973	2973	2961
3.2	2958	2965	2968	2966	2957	2946	2935	2923	2922
3.3	2860	2886	2898	2902	2900	2896	2897	2894	2889
3.4	2758	2800	2828	2842	2850	2857	2859	2857	2853

4. Calculation of the spatial number density

In complete analogy with the method developed by Koschack and Rendtel [4], the spatial number density of particles causing meteors of photographic absolute magnitude at least +3.5 may be obtained from

$$\rho(m \leq +3.5) = \frac{\mathrm{ZHR}_o \times c(r)}{3600 \times A_{\mathrm{red}}(r, h_f, H) \times v_\infty}, \tag{5}$$

where ZHR_o is the observed photographic zenithal hourly rate and v_∞ the geocentric velocity of the shower meteors in km/s. The correction factor c was introduced to account for the loss of meteors due to perception, and is given by

$$c(r) = \frac{\sum_{m=-\infty}^{+3} r^m}{\sum_{m=-\infty}^{+3} r^m \times p_{\mathrm{ph}}(3.5 - m)},$$

where $p_{\mathrm{ph}}(\Delta m)$ represents the probability of perception of a meteor with $\Delta m = plm - m$. When the favorable camera field center is selected, the photograph records any meteor brighter than plm, irrespective of its position on the field. The fact that Δplm is very small across the photograph ensures the validity of the above statement. As a consequence, $p_{\mathrm{ph}}(plm - m) \equiv 1$ while $m \leq plm$, and thus $c(r) = 1$ for any value of the population index.

The photographic zenithal hourly rate can be computed from

$$\mathrm{ZHR}_o = \frac{N}{T} \times \sin^{-1} h_R \times r^{3.5-plm}, \tag{6}$$

where N represents the number of recorded meteors whose beginning points are *inside* the camera field boundaries and T the exposure time of the photograph. Note that the reference photographic meteor limiting magnitude has already been used in $c(r)$ and equation (6).

We further define the flux density Q, related to the spatial number density through

$$Q(m \leq 3.5) = 3600 \times v_\infty \times \rho(m \leq 3.5). \tag{7}$$

The expressions for $Q(M \geq M_0)$ and $\rho(M \geq M_0)$, the flux density and the spatial number density of particles with masses larger than a certain value M_0, respectively, can be taken from [4]. Bearing in mind equations (5) and (6), it is possible to rewrite equation (7) as

$$Q(m \leq 3.5) = \frac{N}{T} \times \sin^{-1} h_R \times \frac{r^{3.5-plm}}{A_{\mathrm{red}}(r, h_f, H)}. \tag{8}$$

There are two different ways to estimate Q from a given set of individual measurements ZHR_i. The first one is averaging the values ZHR_i and obtaining a single value $\mathrm{ZHR}_{\mathrm{av}}$ which allows the calculation of Q. The second method is computing one individual value Q_i from each individual measurement ZHR_i and then averaging these estimates Q_i. Since the flux density depends on h_f through the reduced area A_{red}, the first procedure cannot be applied. Therefore, the best approximation to Q is the average, $\overline{Q}$, of the individual values Q_i. Now we deal with the expected error of $\overline{Q}$, namely $\sigma_{\overline{Q}}$.

Let σ_i be the uncertainty when determining Q_i. The error σ_i comes from the uncertainties associated to each of the variables entering equation (8). The errors σ_N, σ_T, σ_{h_R}, σ_r, σ_{plm}, σ_{h_f}, and σ_H are random, independent errors. Accordingly, the global uncertainty they produce in Q_i is found using the method of the quadratic sums. We are not yet finished, however, since the radiant zenithal-distance correction $C_R \equiv \sin^{-a} h_R$ adds a further error to σ_i. If only a pure geometrical correction is performed, the exponent a turns out to be +1.00. It has been proved however that the decrease of the meteor brightness for large values of h_R modifies a (Roggemans, [14]). From observational data, Zvolánková [15] found $a = +1.47 \pm 0.11$, which agrees well with

the work of Roggemans. Thus, the use of $a = +1.00$ leads to a systematic error in Q_i. The presence of a systematic error strongly affects the computation of $\sigma_{\overline{Q}}$, but, once its value has been estimated, it can be handled with the techniques of the covariance matrix and the theory of error propagation [16]. Notice that there are no other systematic trends as the only possible source for them would be the limiting magnitude correction $C_{plm} \equiv r^{3.5-plm}$ and the recorded range of magnitudes is small enough.

Now suppose that Q_i is affected by a systematic error S_i and a random error σ_i'. Since both errors are independent of each other, it follows from the central limit theorem that the total error σ_i can be obtained by adding the two in quadrature, i.e.

$$\sigma_i = \sqrt{\sigma_i'^2 + S_i^2}\,.$$

Hence, as far as the error of one individual estimate Q_i is concerned, there are no changes from the method of quadratic sums when systematic errors have to be included. It is possible to approximate S_i by

$$S_i \approx \left|\frac{\partial Q_i}{\partial a}\Delta a\right|,$$

where Δa represents the probable uncertainty of the radiant zenithal distance correction exponent a. We may use $\Delta a \approx 0.47$ according [15]. From equation (8) one thus obtains

$$S_i \approx Q_i \Delta a \ln(\sin^{-1} h_{R_i}). \tag{10}$$

The numerical values of T, h_R, and h_f can be known with high accuracy, and so the errors σ_T, σ_{h_R}, and σ_{h_f} produce negligible contributions to σ_i'. The other sources of error are σ_N, σ_r, σ_{plm}, and σ_H. Thus we have

$$\sigma_i' = \sqrt{\left(\frac{\partial Q_i}{\partial N_i}\sigma_{N_i}\right)^2 + \left(\frac{\partial Q_i}{\partial r_i}\sigma_{r_i}\right)^2 + \left(\frac{\partial Q_i}{\partial plm_i}\sigma_{plm_i}\right)^2 + \left(\frac{\partial Q_i}{\partial H_i}\sigma_{H_i}\right)^2}. \tag{11}$$

From equation (8), one finds

$$\frac{\partial Q_i}{\partial N_i} = \frac{Q_i}{N_i};$$

$$\frac{\partial Q_i}{\partial r_i} = \frac{\partial Q_i}{\partial\left(\frac{r^{3.5-plm_i}}{A_{\mathrm{red}_i}}\right)}\frac{\partial\left(\frac{r^{3.5-plm_i}}{A_{\mathrm{red}_i}}\right)}{\partial r_i} = (3.5 - plm_i)\frac{Q_i}{r_i} + \frac{Q_i}{A_{\mathrm{red}_i}}\left|\frac{\partial A_{\mathrm{red}_i}}{\partial r_i}\right|;$$

$$\frac{\partial Q_i}{\partial plm_i} = Q_i \ln r_i;$$

$$\frac{\partial Q_i}{\partial H_i}\sigma_{H_i} = \frac{\partial Q_i}{\partial A_{\mathrm{red}_i}}\frac{\partial A_{\mathrm{red}_i}}{\partial H_i}\sigma_{H_i} = -\frac{2Q_i}{A_{\mathrm{red}_i}}\varepsilon A_{\mathrm{red}_i} = -2Q_i\varepsilon,$$

where $\varepsilon = 0.08$ for $H = (100 \pm 9)$ km, $\varepsilon = 0.025$ for Perseids ($H = (114 \pm 3)$ km), and $\varepsilon = 0.06$ for Leonids ($H = (118 \pm 6)$ km). While the random fluctuations in the number of meteors N can be accounted for by using a Poisson distribution, i.e., $\sigma_N = \sqrt{N}$, the errors σ_r and σ_{plm} must be obtained from global analyses and experiments, respectively. With regard to $\partial A_{\mathrm{red}}/\partial r$, the data given in Tables 4–6 should be sufficient. Combining the previous results and equation (9), the standard deviation σ_i of the estimate Q_i becomes

$$\sigma_i = Q_i\sqrt{\frac{1}{N_i} + \left(\frac{3.5 - plm_i}{r_i} + \frac{\left|\frac{\partial A_{\mathrm{red}_i}}{\partial r_i}\right|}{A_{\mathrm{red}_i}}\right)^2\sigma_{r_i}^2 + \sigma_{plm_i}^2 \ln^2 r_i + 4\varepsilon_i^2 + \left(\frac{S_i}{Q_i}\right)^2}. \tag{12}$$

The flux density $Q(m \leq 3.5)$ must be computed as the weighted mean of the individual measurements Q_i, i.e.,

$$\overline{Q} = \frac{\sum_i \frac{Q_i}{\sigma_i^2}}{\sum_i \frac{1}{\sigma_i^2}}$$

The values Q_i are not mutually independent since they share a systematic error coming from the uncertainty of the zenithal radiant distance correction. As a consequence, the standard deviation $\sigma_{\overline{Q}}$ of $\overline{Q}$ is given by

$$\sigma_{\overline{Q}}^2 = \sum_j \left(\frac{\partial \overline{Q}}{\partial Q_j} \sigma_j \right)^2 + 2 \sum_j \sum_{k>j} \frac{\partial \overline{Q}}{\partial Q_j} \frac{\partial \overline{Q}}{\partial Q_k} \operatorname{cov}(Q_j, Q_k), \tag{13}$$

where $\operatorname{cov}(Q_j, Q_k)$ represents the covariance of Q_j and Q_k, i.e., the degree of correlation between Q_j and Q_k introduced by Δa. The values Q_j and Q_k have systematic errors S_j and S_k and also random errors σ_j' and σ_k'. This feature can be treated by considering Q_j as having two parts, Q_j^R with random error σ_j' and Q_j^S with systematic error S_j. The same applies to Q_k. By this definition, Q_j^R and Q_k^R are independent of each other and of Q_j^S and Q_k^S, whereas Q_j^S and Q_k^S are completely correlated. It can be shown [16] that $\operatorname{cov}(Q_j, Q_k) = \operatorname{cov}(Q_j^S, Q_k^S) = S_j S_k$ or, by virtue of equation (10),

$$\operatorname{cov}(Q_j, Q_k) = Q_j Q_k (\Delta a)^2 \ln(\sin^{-1} h_{R_j}) \ln(\sin^{-1} h_{R_k}).$$

The partial derivatives entering equation (13) read

$$\frac{\partial \overline{Q}}{\partial Q_j} = \frac{1}{\sum_i \frac{1}{\sigma_i^2}} \frac{1}{\sigma_j^2},$$

whence

$$\sum_j \left(\frac{\partial \overline{Q}}{\partial Q_j} \right)^2 \sigma_j^2 = \frac{1}{\sum_i \frac{1}{\sigma_i^2}},$$

and thus

$$\sigma_{\overline{Q}}^2 = \frac{1}{\sum_i \frac{1}{\sigma_i^2}} \left(1 + \frac{2(\Delta a)^2}{\sum_i \frac{1}{\sigma_i^2}} \sum_j \sum_{k>j} \frac{Q_j Q_k}{\sigma_j^2 \sigma_k^2} \ln(\sin^{-1} h_{R_j}) \ln(\sin^{-1} h_{R_k}) \right). \tag{14}$$

If $\Delta a = 0$, i.e., if the error due to the uncertainty of the radiant zenithal distance is neglected, equation (14) provides the usual standard deviation of a weighted mean in which all the errors are independent. But in general $\Delta a \neq 0$. While the net effect of random errors decreases in size when the number of measurements increases, the effect of systematic errors does not fall off at all.

Equation (14) implies that, for a sufficiently large set of individual measurements Q_i, the error $\sigma_{\overline{Q}}$ is dominated by the systematic error that stems from Δa. The only way to improve $\sigma_{\overline{Q}}$ is reducing the uncertainty Δa. This will require more research work and a firm determination by the *IMO* to change the standard procedure if necessary. Meanwhile, the only possibility to keep $\sigma_{\overline{Q}}$ as low as possible is to observe with $h_R \approx 90°$, since in that case the covariance of any pair of individual estimates Q_j and Q_k becomes nearly zero (cfr. equation (10)).

If spatial number densities are sought instead of flux densities, the above procedure still applies. The uncertainty $\sigma_{\overline{\rho}}$ is then given by $\sigma_{\overline{\rho}} = \sigma_{\overline{Q}} / 3600 v_\infty$, which comes directly from equation (7).

5. Conclusions

The method given above permits the determination of both spatial number densities and flux densities from photographic records. Only slight changes have had to be made to the visual procedure of Koschack and Rendtel [4] to make it applicable to photography. The presence of a systematic error coming from the radiant zenithal distance correction must be investigated more thoroughly, since it also affects the analysis of visual data. The current *IMO* method does not treat systematic errors and, although the whole computations may look nice, the results can be a complete disaster if they are not properly accounted for.

Appendix

We devote this Appendix to the computation of $A_{\text{red}}(h_f)$. A rectangular coordinate system with origin at the camera lens is selected for further use. The z-axis points towards the zenith, while the y-axis is directed along the projection of the azimuth of the camera field center onto the perpendicular plane to the z-axis. In this reference frame, the meteor layer may be described by an spherical surface with equation

$$x^2 + y^2 + (z + 6371 \text{ km})^2 = (6371 \text{ km} + H)^2, \tag{15}$$

where H represents the height of meteor appearances.

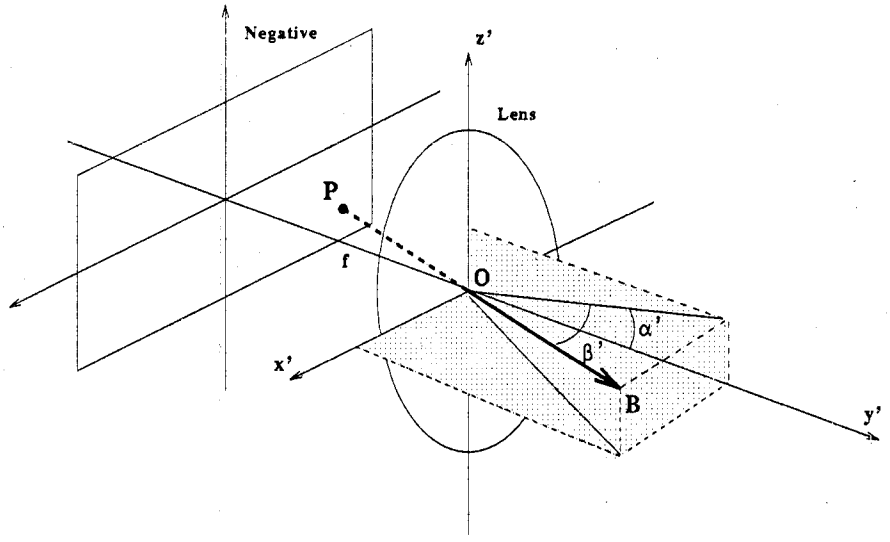

Figure 2 – Diagram of a camera. The y'-axis represents the projection of the camera field center. Point P on the negative is specified by angles α' and β' or, equivalently, by vector $\overline{OB}$.

The aim is to calculate the geometrical projected area A_i of a small zone of the photograph. Figure 2 shows a diagram of the camera. Any point P on the negative is specified by two angles α' and β' whose maximum values are 13°.5 and 19°.8 respectively. Both angles define the positional vector $\overline{OB}$ as

$$\begin{aligned} x' &= R \sin \beta'; \\ y' &= R \cos \beta' \cos \alpha'; \\ z' &= R \cos \beta' \sin \alpha', \end{aligned} \tag{16}$$

where $R = |OB|$.

Now suppose that the camera field center has an altitude h_f above the horizon (xy-plane). This is equivalent to the rotation of the z'- and y'- axes around the x'-axis by an angle of $-h_f$ (see Figure 3, *left*). The coordinates of vector $\overline{OB}$ in the xyz-system are thus obtained via the matrix of the rotation, i.e.,

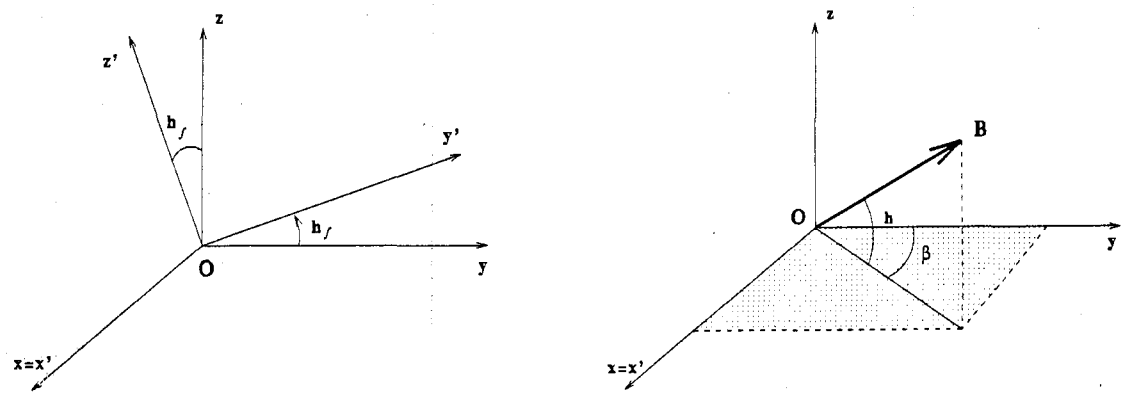

Figure 3 – *Left*: Position of the camera's coordinate system presented in Figure 2 with respect to the xyz-system when the camera field center is aimed at angle h_f above the horizon. *Right*: Definition of angles h and β for vector $\overline{OB}$. Angle h represents the elevation of point P above the horizon (xy-plane).

$$\begin{pmatrix} x \\ y \\ z \end{pmatrix} = \begin{pmatrix} 1 & 0 & 0 \\ 0 & \cos h_f & -\sin h_f \\ 0 & \sin h_f & \cos h_f \end{pmatrix} \begin{pmatrix} x' \\ y' \\ z' \end{pmatrix}, \tag{17}$$

whence

$$\begin{aligned} x &= R \sin \beta'; \\ y &= R \cos \beta' \cos (\alpha' + h_f); \\ z &= R \cos \beta' \sin (\alpha' + h_f). \end{aligned}$$

Writing $h' \equiv \alpha' + h_f$, the parametrical form (p being the parameter) of the straight line defined by vector $\overline{OB}$ becomes

$$\begin{aligned} x &= p \frac{\tan \beta'}{\cos h'}; \\ y &= p; \\ z &= p \tan h'. \end{aligned} \tag{18}$$

It is now easy to solve equations (15) and (18), which gives the projection of point P onto the meteor level. The whole photograph is sampled by letting α' run from $-13\overset{\circ}{.}5$ to $+13\overset{\circ}{.}5$ and β' from $-19\overset{\circ}{.}8$ to $+19\overset{\circ}{.}8$. (Note the symmetry, which means that we only have to consider $0^\circ \leq \beta' \leq 19\overset{\circ}{.}8$.)

The last important parameter is the altitude h of vector $\overline{OB}$ above the horizon, since it provides the extinction ε associated to P. From Figure 3, *right*, and formulae (18), one obtains

$$\begin{aligned} h &= \arctan(\tan h' \cos \beta); \\ \beta &= \arctan \left(\frac{\tan \beta'}{\cos h'} \right). \end{aligned} \tag{19}$$

The method to compute A_{red} for a given camera center altitude h_f works then as follows:

1. The negative is discretized on a mesh of points separated by $0\overset{\circ}{.}02$. Four of these points define a small square that will be projected onto the meteor level to obtain the corresponding geometrical area A_i.
2. The projection of the vertices of each square using equations (15) and (18) produces a trapezoid at the meteor level. The coordinates of the trapezoid vertices are (x_i, y_i, z_i) with $i = 1, \ldots, 4$. Since the grid step is small enough, the trapezoid can be approximated by a

rectangle. The area A_i is thus the product of the length of two of its adjacent edges. In order to minimize the error, A_i is taken as the arithmetic mean of the two possible products $l_1 \times l_2$ and $l_3 \times l_4$. Accordingly, ΔA_i is the maximum difference between A_i and $l_1 \times l_2$ or $l_3 \times l_4$.

3. The distance d_i from the camera to the trapezoid is computed. By applying formula (19) we get the altitude above the horizon and select the relevant extinction value.
4. The geometrical area A_i is corrected for distance and extinction.
5. The whole procedure runs until all the squares on the negative have been projected. Finally, the results are summed up to obtain A_{red}.

As an example, Figure 5 shows the camera field boundaries at the meteor level when $h_f = 50°$ and $H = 100$ km (only xy-coordinates are shown).

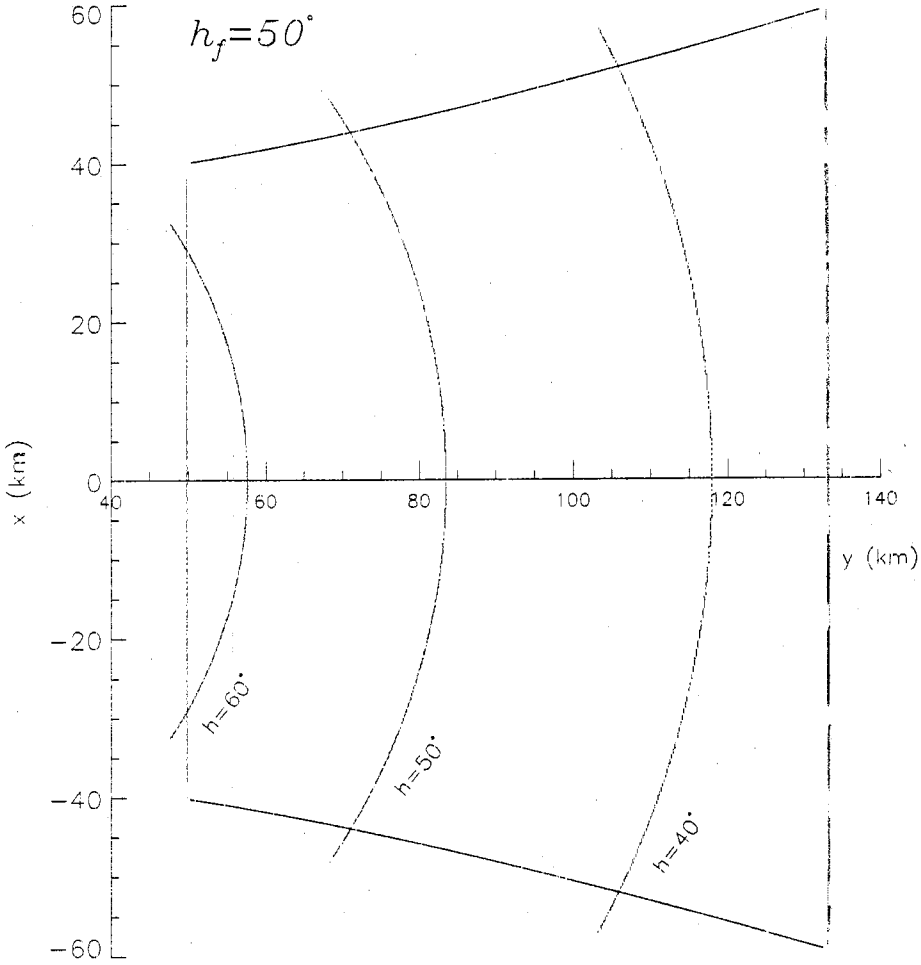

Figure 4 – Projection of the camera field boundaries onto the meteor level for $h_f = 50°$ and $H = 100$ km. We assume a 35 mm, $f = 50$ mm camera with the longest edge of the photograph parallel to the horizon.

Acknowledgments

Many people contributed to the development of the photographic technique. Among them, we must cite Josep M. Trigo, Ralf Koschack and Jürgen Rendtel. Some of the topics discussed in Sections 2 and 3 were first put forward by these meteor workers and were never published. I am indebted to Robert Hawkes and Jürgen Rendtel for their useful comments to the paper. I also appreciate the help of Mark Kidger, who corrected the English of the manuscript and discussed several points concerning the whole procedure. David Asher is warmly acknowledged for making available some important references.

References

[1] L.R. Bellot, "On the Presence of Trains in Meteor Showers", *WGN* 20:3, June 1992, pp. 140–144.

[2] M. Vints, "Meteor Trains", in *Proceedings of the 1991 IMC*, J. Rendtel and R. Arlt, Eds., Potsdam, Germany, 1992, pp. 56–58.

[3] J. Rendtel, *personal communications*, 1994.

[4] R. Koschack and J. Rendtel, "Determination of Spatial Number Density and Mass Index from Visual Meteor Observations", *WGN* 18:2 and 18:4, April and August 1990, pp. 44–58 and 119–140.

[5] J. Rendtel, "Handbook for Photographic Meteor Observations", IMO Monograph 3, 1993.

[6] D.F. Malin, "Photography in Astronomy", *Phys. Bull. (U.K.)* 33, pp. 206–210.

[7] R. Arlt, "The Software Radiant", *WGN* 20:2, April 1992, pp. 62–69.

[8] R. Koschack, R. Hawkes, "Observations During Exceptionally High Activity", *WGN* 21:3, June 1993, pp. 92–94.

[9] J.M. Trigo, "Determination of Spatial Number Density from Photography", in *Proceedings of the 1993 IMC*, P. Roggemans, Ed., Puimichel, France, 1994, pp. 77–84.

[10] J. Bartels, P. ten Bruggencate, "Landolt–Börnstein. Astronomie und Geophysik", Springer-Verlag, 1952, p. 33.

[11] G.J. Jacchia, F. Verniani, R.E. Briggs, "An Analysis of the Atmospheric Trajectories of 413 Precisely Reduced Photographic Meteors", *Smithson. Contrib. Astroph.* 10:1, 1967, pp. 1–139.

[12] T. Sarma, J. Jones, "Double-station Observations of 454 TV Meteors", *Bull. Astron. Inst. Czechosl.* 36, 1985, pp. 9–24.

[13] R.E. McCrosky, A. Posen, "Orbital Elements of Photographic Meteors", *Smithson. Contrib. Astroph.* 4:2, 1961, pp. 15–84.

[14] P. Roggemans, "Perseids 1985 and the Zenith Distance Correction", *WGN* 14:5, October 1986, pp. 149–152.

[15] J. Zvolánková, "Dependence of the Observed Rate of Meteors on the Zenith Distance of the Radiant", *Bull. Astron. Inst. Czechosl.* 34, 1983, pp. 122–128.

[16] R.J. Barlow, "Statistics. A Guide to the Use of Statistical Methods in the Physical Sciences", John Wiley and Sons, 1989, pp.59–66.

Received April 1994; revised June 1994; accepted July 1994.

Fireballs and Meteorites

Fireball

Germany-Austria, May 25, 1994, $21^h28^m \pm 1^m$ UT

Pavel Spurný, Ondřejov Observatory, and Dieter Heinlein

On the night of May 25, 1994, a very slow-moving fireball of approximately −12 maximum absolute magnitude was photographed by two German and two Czech stations of the European Fireball Network.

A very slow-moving and long duration fireball of minus twelve maximum absolute magnitude was photographed by two German and two Czech stations of the European Fireball Network on the night of May 25, 1994. The fireball traveled a 240-km luminous trajectory in 18.7 seconds and terminated its light at a height of 46.5 km. The slope of the fireball trajectory to the Earth's surface was only 7°, which means that the trajectory was almost horizontal.

The following results are based on all available records. Time of the fireball passage was taken from the visual observation.

Table 1 – Trajectory data.

	Beginning	Maximum light	Terminal
Velocity (km/s)	15.63 ± 0.03	13.92	8 ± 1
Height (km)	79.4 ± 1.6	63.4	46.5 ± 0.3
Latitude (° N)	48.705 ± 0.012	48.12	47.478 ± 0.002
Longitude (° E)	9.011 ± 0.013	10.27	11.585 ± 0.003
Abs. magnitude	− 1.9 ± 1.2	−11.7 ± 0.8	− 4.0 ± 1.2
Photomet. mass (kg)	100	80	less than 0.1
Z R (°)	81.06 ± 0.14		83.17 ± 0.14

Fireball type: IIIA
Ablation coefficient: (0.225 ± 0.004) s^2/km^2

Table 2 – Radiant data.

Radiant (2000.0)	Observed	Geocentric	Heliocentric
α (°)	103.0 ± 0.3	93.0 ± 0.3	
δ (°)	+ 29.07 ± 0.14	+15.5 ± 0.2	
λ (°)			138.06 ± 0.07
β (°)			− 02.49 ± 0.06
Initial velocity (km/s)	15.70 ± 0.03	11.43 ± 0.04	36.29 ± 0.05

Table 3 – Orbital data.

Orbit (2000.0)	
a	2.042 ± 0.018 AU
e	0.560 ± 0.003
q	0.8983 ± 0.0012 AU
Q	3.19 ± 0.03 AU
ω	313°.2 ± 0°.3
Ω	244°.5256 ± 0°.0007
i	2°.60 ± 0°.06

Ongoing Meteor Work

The Makings of Meteor Astronomy: Part VII

Martin Beech, University of Western Ontario

The idea that meteors might be some form of "electrical manifestation" was a popular one for several decades near the end of the 18th century. The great fireball of August 18, 1783, prompted one researcher, Charles Blagden, to develop a detailed empirical model which described all manner of meteoric phenomena.

1. Preamble: fads, fashions, and synthesis

We have noted in previous instalments of this series that science has had its many fads and fashions. There are also many examples in the history of science where researchers have "pick-up" new discoveries or ideas and then, in an apparent fit of enthusiasm, attempted to describe all unexplained phenomena in terms of the new discovery. Black holes would be an example of an astronomical "fad object" in the sense that they have been invoked, at one time or another, to explain a myriad of astronomical phenomena. These same phenomena, it often turns out, have later been explained by less exotic means. Towards the close of the 18th century, the new scientific fad was electricity.

Not only do scientists like to use new discoveries and ideas in their work, they also like to synthesize. That is, it is often said that the mark of a "good theory" is that it can explain a large number of apparently diverse phenomena with a minimum of hypothesis. This is exactly what Charles Blagden (1748–1820) attempted to do [1] when he published a report to the Royal Society [2] on the appearance of the great fireball of August 18, 1783.

2. All manner of electrical phenomena

The pioneering studies on meteor origins made by Edmund Halley and John Pringle [3] in the first half of the 18th century did not greatly influence the prevalent ideas on meteor origins. This is exemplified by the description of meteors given in the 1771 edition of the *Encyclopaedia Britannica*. The account given in the Encyclopaedia is essentially the Aristotelean hypothesis as modified by Isaac Newton [4]. The text explains, *meteors are of three kinds; fiery, airy, and watery. Fiery meteors consist of a fat sulfurous smoke set on fire; such as falling stars, draco volans, the igneus fatus, and other phenomena, appearing in the air.*

In his account and discussion of the August 18, 1783, fireball, Blagden attacks both the Aristotelean hypothesis (as outlined by Halley in his 1719 paper) and the extra-terrestrial hypothesis (as outlined by Pringle in his 1759 paper). Of the former he notes, *Dr. Halley gives no just explanation of the nature of these vapors, nor of the manner in which they can be raised, ..., nor does he account for the regular arrangement in a straight and equable line of such prodigious extent, or for their continuing to burn in such rarefied air.*[1] Of the latter hypothesis Blagden notes, *most observers describe the meteors, not as looking like solid bodies, but rather like a fine luminous matter, perpetually changing shape and appearance ... I think whoever carefully peruses the various accounts of fireballs ... will perceive that these phenomena do not correspond with the idea of a solid nucleus.*

Interestingly, Blagden also advances the argument that the bright meteors cannot be solid bodies because it would be expected that, on occasion, some fragment of their constituent material would fall intact to the ground. Blagden made his comments 19 years before the well documented fall of meteoric stones at L'Aigle in France, and, in this respect, he was essentially reflecting the wisdom of the day—stones do not fall from the sky.

[1] Blagden also raised a very simple, and yet powerful observational argument against Halley's "train of vapors hypothesis." *Would it not be expected*, Blagden argued, *that such trains would sometimes take fire in the middle, and so present the phenomenon of two meteors at the same time, receding from one another in a direct line?* This is one of those questions that, once raised, is so obvious that it is a wonder no one thought of it earlier.

Another interesting argument that Blagden leveled against the extra-terrestrial hypothesis was that concerned with the observed velocities. He argued, *a body falling from infinite space towards the earth would have acquired a velocity of no more than 7 miles a second, when it came within 50 miles of the Earth's surface, where as the meteors seem to move at least three times faster.* This argument is in fact flawed in the sense that Halley had not suggested that the extra-terrestrial (i.e., meteoric) matter had accumulated with zero velocity, and further, Blagden seems to have forgotten that the Sun would be the main gravitational "attractor" for an object falling from infinity.

Having dismissed both the extra-terrestrial solid-body, and the igniting vapors hypothesis, Blagden had cleared the way for his own ideas on the meteoric phenomena. He wrote the following:

> *what then can these meteors be? The only agent in nature with which we are acquainted that seems capable of producing such phenomenon is electricity. I do not mean that, by what is already known of the fluid, all the difficulties relative to meteors can be solved, as the laws, by which its motions on a large scale are regulated in those regions so nearly empty of air, can scarcely, I imagine, be investigated in small experiments with exhausted vessels, but only that several of the facts point out a near connection and analogy with electricity, and that none of them are irreconcilable to the discovered laws of that fluid.*

From a phenomenological point of view, Blagden could present a good argument for his hypothesis, and in particular he noted, *electricity moves with such a prodigious velocity as to elude all the attempts hitherto made by philosophers to detect it; but the swiftness of meteors, stating it at 20 miles a second, is such as no experiments yet contrived could have discovered, and which seems to belong to electricity alone.* Further to this, however, Blagden also argues that there is good observational evidence to link the bright fireballs with the aurora, or northern lights, a phenomena that Edmund Halley had previously explained in terms of magnetic fluids [4].

Blagden wrote, *the electrical origin of meteors is deduced from their connection with the northern lights, and the resemblance they bear to these electrical phenomena ... in my opinion, the most remarkable analogy of all, and that which tends most to elucidate the origin of these meteors, is the direction of their course, which seems, in the very large ones at least, to be constantly from or towards the north or north-west quarter of the heavens, and indeed approach very nearly to the present magnetic meridian.* Developing his argument further, Blagden noted, *whether their motion shall be from the northern quarter of the heavens or toward it ... I consider them in the former case as masses of the electric fluid repelled, or bursting from the great collected body of it in the north; and in the latter case, as masses attracted towards the accumulation.* Blagden's argument is based on small number statistics, and as we know today is clearly not true. However, it is one of those strange quirks of history that most of the bright fireballs investigated during the 17th and 18th century moved as Blagden described.

The fireball model proposed by Blagden was in fact part of a grand synthesis which attempted to explain all (fiery) meteoric phenomena. The essential factor that governed the appearance of the various electrical manifestations was atmospheric height. Blagden explains as follows:

> *... distinct regions are allotted to the various electrical phenomena of our atmosphere. Here below we have thunder and lightning, from the unequal distribution of the electrical field among the clouds, in the loftier regions, ..., we have the various gradations of falling stars, till beyond the limits of our crepuscular atmosphere the fluid is put into motion in sufficient masses to hold a determined course and exhibit the different appearances of what we call fire-balls; and probably at a still greater elevation above the earth, the electricity accumulates in a lighter less condensed form to produce the wonderful diversified streams and coruscations of the aurora borealis.*

The shooting stars are placed in a lower region of the atmosphere in Blagden's model. This is so because he observed that they do not obey the north-south motion ascribed to fireballs, and

because they have *a swifter apparent motion.* Blagden also reasoned that the *electric fluid* of the shooting stars was *more divided in [the] more resisting air* of the lower atmosphere and thus *more exposed to the action of extraneous causes.*

3. Closing comments

Blagden was not the first researcher to suggest that fireballs might be electrical manifestations. The French philosopher Jean-Baptiste Le Roy, for example, had made the suggestion that electricity was the "cause" of the fireball seen over Southern England and Northern Europe on July 17, 1771. Unlike Blagden after him, however, Le Roy argued that there was no connection between fireballs and the aurora [5]. His main argument against there being any such connection was that fireballs traveled in all directions and appeared in all seasons.

While the idea that meteors might have an electrical origin persisted well into the 19th century (and even the 20th), a new set of arguments in favor of the extra-terrestrial hypothesis was put forward during the 1790s. The arguments presented in the final decade of the 18th century proved extremely important to the development of meteor astronomy. We shall begin to investigate the events of that crucial decade next time.

References

[1] M. Beech, *Jour. British Astron. Assoc.* 99:3, 1989, p. 130.
[2] C. Blagden, *Philos. Trans. Roy. Soc. London* 74, 1784, p. 201.
[3] M. Beech, *WGN* 22:2, 1994.
[4] M. Beech, *WGN* 21:6, 1993.
[5] J.G. Burke, in *Cosmic Debris: Meteorites in History*, California University Press, Berkeley, 1986.

Moving Ripples in Solar Haloes—Update

Alastair McBeath

Three sightings of moving ripples crossing solar halo phenomena not previously widely-known are reported. This brings the total of such events observed to seven.

1. Introduction

In 1993, I issued a call for observations of moving ripples in solar haloes in *WGN* [1], and other publications, since if these features are the result of acoustic sound waves from meteors, enhanced activity from the Perseid shower in 1993 August might well have produced further such events. So far, no sightings have been reported as a result of that shower at least. However, three other observations of moving ripples have come to light, and several groups or individuals have expressed an interest in keeping watch for future sightings, particularly in Finland and Germany. It is to be hoped that the numbers of observed ripple phenomena will increase in the near future.

2. Observations

The first of the new sightings was made at around 13^h00^m UT on September 7, 1976, when fast moving ripples were seen in the anti-sun direction on a parhelic circle. This observation was made by four observers, Elaine Allchin, Tim Allchin, Bob Cripps, and Sue Haywood, who were on board a barge on the Oxford Canal near Bridge 74 (approximately 5 km south east of the town of Rugby, Northamptonshire, England, $\lambda \approx 1°15'$ W, $\varphi \approx 52°20'$ N) at the time. Figure 1 is a reproduction of the original drawing made by Haywood, which shows where the ripples were seen, and what halo phenomena were observed during the course of the day.

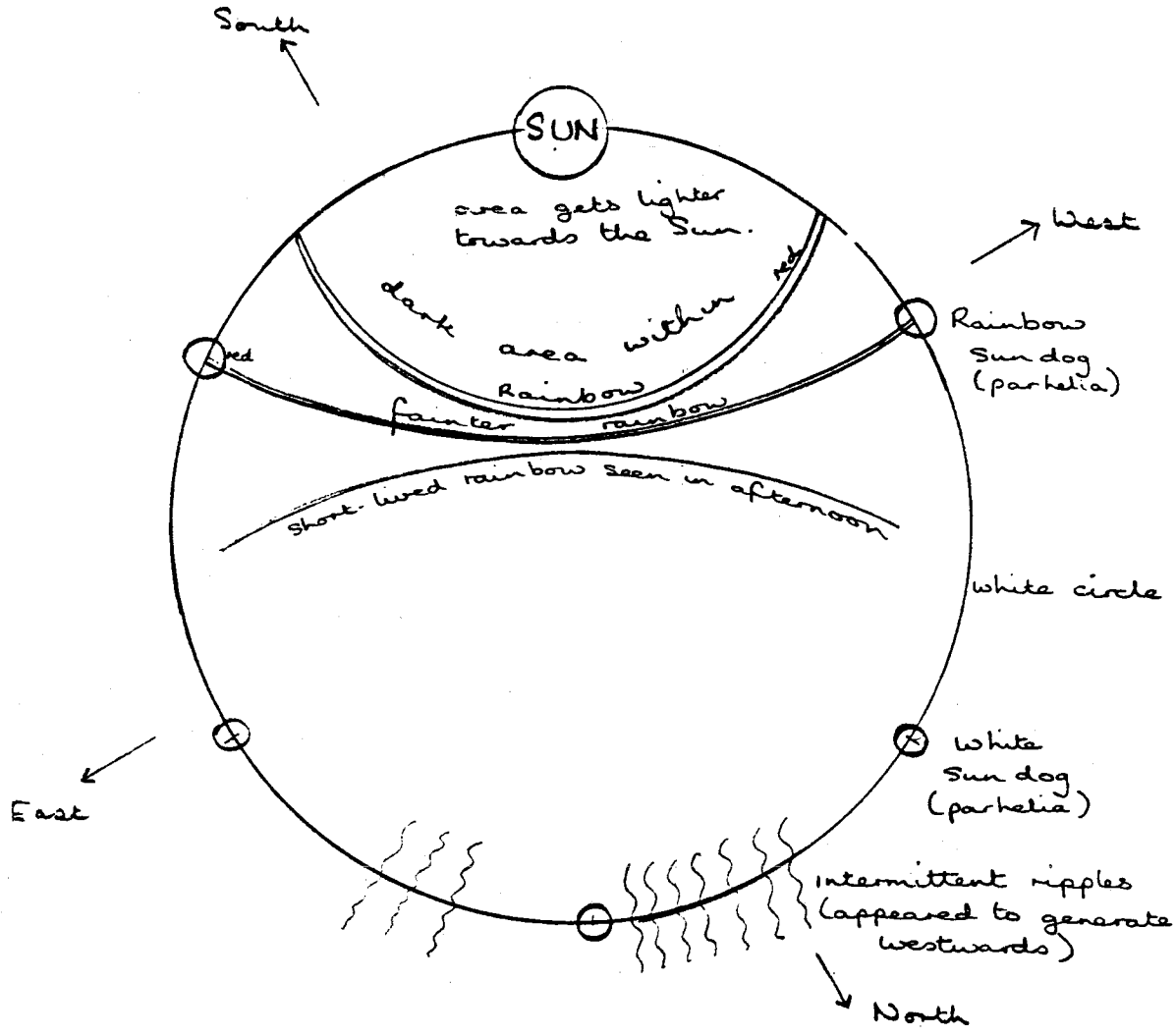

Figure 1 – A reproduction of the halo and ripple display drawn by Haywood, September 7, 1976.

The written report also produced by Haywood is reprinted verbatim below [2]:

> *While relaxing in the sunshine after lunch, Elaine saw a rainbow. We all looked up, and were rewarded by the following. (There were high fine misty clouds, drawn out by the wind).*
>
> *When first observed, at* $12^{h}45^{m}$ *GMT, the Sun was the center of radius of an arc of rainbow. The Sun itself was on a large white circle. The first sun dog seen was opposite the Sun, and was white, as were the two* 60° *either side of it. These three, and the white circle faded and returned (not all together) more than once. The two rainbow sun dogs were more persistent, as was the rainbow itself. These latter were joined by another rainbow, tangential to the other, and appearing to join the dog. The rainbow and rainbow dogs were visible until sunset. Just before* $13^{h}00^{m}$*, fast moving ripples were seen across the white circle.*

Without trying to explain all the phenomena seen on September 7, 1976, though it is obvious several refraction haloes (the "rainbow"-colored features referred to above) and one reflection halo (the "large white circle") were present, the description makes it clear that the ripples were seen only in the white parhelic circle, and that the halo effects were almost certainly in high-altitude cirrus or cirro-stratus clouds (the note of "high fine misty clouds, drawn out by the wind" is an accurate description of cirrus "mare's tail" clouds).

The observation tallies well with others of the ripple effect, except that this example suggests the ripples occurred in ordinary tropospheric clouds, unlike the aircraft contrails of the previous four sightings.

The second new sighting was made by Jürgen Rendtel on April 15, 1988, at around 8^h34^m UT from Schönefeld near Berlin, Germany ($\lambda \approx 13\overset{\circ}{.}5$ E, $\varphi \approx 52\overset{\circ}{.}5$ N), when moving ripples were seen for a short time in a sundog to the western side of the Sun [3]. Again, this observation of the ripple effect was seen in "ordinary" cirro-stratus clouds, not in a contrail. Rendtel calls into question whether the sound from meteors could be propagated through the atmosphere as described by Archenhold [4], but Archenhold has concluded that the intensity of the sound from a meteor would decrease, not as the square of the distance from the meteor's path, but linearly. He was not able to compute the exact shape of the wavefront that would be produced, however [4,5].

Finally, the most recent observation was made by Peter-Paul Hattinga Verschure from Arnhem, the Netherlands ($\lambda \approx 5\overset{\circ}{.}9$ E, $\varphi \approx 52\overset{\circ}{.}0$ N), on August 17, 1988, when moving ripples were seen in a 120° parhelia on a parhelic circle. This was to the north-north-west of the Sun. Several other refraction haloes were seen at the same time, so once more, this sighting seems to have been made in cirro-stratus clouds, not a contrail. The ripples moved from north to south, in the general direction of (although not directly towards) the Sun [6].

3. Conclusion

Although this current paper has increased the number of reported sightings of moving ripples seen in solar haloes to almost twice what already existed, more observations are badly needed, especially by instrumental techniques.

It is also important that any other previously-made but so far still unknown reports should be brought to light as soon as possible. It is worrying that Cripps reports his submission of the 1976 sighting was forwarded to several authorities in Britain soon after it was made, but that no one bothered to record or explain the phenomenon [2]. Consequently, there was a good chance that but for this present appeal for data, this observation might have been permanently lost. In order to examine more fully the potential causes of this effect, it is vital that anyone seeing such moving ripples, or coming across other reports of them elsewhere should make them more widely-known. If anyone reading this is aware of any other outstanding observations, please contact me with details.

Acknowledgments

I should particularly like to thank Bob Cripps and Jürgen Rendtel for the communication of their sightings, as well as the three other observers who reported the 1976 event, and also Teemu Hankamäki who sent a copy and translation from the Finnish of the Hattinga Verschure sighting. I am furthermore very grateful to Gunter Archenhold for several fascinating discussions of this phenomenon since 1984.

References

[1] A. McBeath, *WGN* 21:3, June 1993, p. 86.
[2] B. Cripps, *personal communications*, 1993.
[3] J. Rendtel, *Die Sterne* 65:1, 1989, pp. 58–59.
[4] G.H. Archenhold, *Quarterly Journal of the Royal Astronomical Society* 25, 1984, pp. 122–125.
[5] G.H. Archenhold, *personal communications*, 1994.
[6] P.-P. Hattinga Verschure, *Ursa Minor* 2, 1989, pp. 22–23.

Multi-Station TV Observations of the 1993 Perseids

S. Suzuki, T. Yoshida, K. Suzuki, and T. Akebo

We calculated the trajectories and orbital elements of 34 Perseids on August 11-12, 1993. The mean radiant position is $\alpha = 47.^\circ8$, $\delta = 57.^\circ5$, at solar longitude $\lambda_\odot = 139.^\circ6$ (2000.0). The mean velocity is $V_g = 58.6$ km/s. The mean height is $H_b = 111.8$ km, $H_e = 96.4$ km. The mean magnitude of the 34 meteors is 4.3.

A strong display of the Perseids in 1991 was observed by double-station TV observations at the *Damine Meteor Observatory (DMO)* in Japan. In 1993, more than 100 meteors were recorded on video tapes at 4 stations of the DMO group. The trajectories and orbital elements of 51 meteors were calculated for the equinox 2000.0.

On August 11 and 12 UT, 1993, TV observations of the *DMO* group were performed with MCP image intensifiers and CCD cameras set up equatorially. The occurrence of the meteors was recorded on an NTSC video cassette recorder (VCR). For image processing, video frames were digitized (512×512 pixels), measured, and calculated by a personal computer. The observational data are listed in Table 1. Observational systems and PC systems are given in Table 2 (K. Suzuki et al., [1]). From 15 to 30 reference stars were measured to determine the position of the meteors. The positional error was about 1′. The spectral response of our systems was approximately near-infrared.

Table 1 – Observational data of the 1993 Perseid TV observations.

Observer	Location	Date	Begin	End	Met.	Lm	Per	Lens	Field
T. Yoshida	$\lambda = 137°31'48''$ E	Aug 11	13^h43^m	19^h42^m	123	11	23	135 mm	8 × 6
	$\varphi = 35°03'54''$ N	Aug 12	13^h20^m	19^h27^m	102	11	44	135 mm	8 × 6
S. Suzuki	$\lambda = 137°30'15''$ N	Aug 11	13^h01^m	19^h11^m	248	10	59	85 mm	13 × 11
	$\varphi = 34°54'29''$ N	Aug 12	13^h00^m	19^h15^m	274	10	126	85 mm	13 × 11
K. Suzuki	$\lambda = 137°19'26''$ N	Aug 11	14^h06^m	19^h10^m	135	10	27	135 mm	10 × 10
	$\varphi = 34°48'47''$ E	Aug 12	13^h00^m	18^h00^m	92	9	38	135 mm	10 × 10
T. Akebo	$\lambda = 137°13'28''$ E							85 mm	16 × 16
	$\varphi = 34°54'38''$ E								

Table 2 – Systems used for the observations.

Observer	Lens	Im. Int.	Video camera	PC	Digitizing
T. Yoshida	135/2.0	V1366P	WV-BD400	EPSON286 (80286)	512 × 512 pxls
S. Suzuki	80/1.2	V1366P	WV-BD400	FM-TOWNS (80386)	512 × 512 pxls
K. Suzuki	135/2.0	V1366P	GR-S95	FM-TOWNS (80386)	512 × 512 pxls
T. Akebo	80/1.4	V1366P	AG-400		

Trajectory parameters of 51 meteors were calculated by my PC with software programmed by Mr. Ueda (whom we kindly acknowledge), and a further selection of 34 meteors was made. Their data are listed in Table 3. When the meteor was observed by 3 or 4 stations, we listed the widest set of observation of the angle Q in Table 3. The symbols have the following meaning: date and time are given in UT; α and δ refer to the radiant position (eq. 2000.0) corrected for zenith attraction and diurnal aberration; V_g is the pre-atmospheric geocentric velocity corrected for deceleration in km/s; $h_{\rm beg}$ and $h_{\rm end}$ are the heights of begin and end of the meteor in km; Q is the angle between the great circles on which the meteor traveled as seen from two stations; SD_1 and SD_2 are the standard deviation of the error in the measurement of the reference stars; and m is the apparent magnitude of the meteor, estimated by comparison with nearby stars.

Figure 1 shows the radiant point distribution on August 11 and 12 (UT). But there are also non-Perseid radiant points. The mean radiant point is given by $\alpha = 47.^\circ8 \pm 2.^\circ4$, $\delta = 57.^\circ5 \pm 1.^\circ0$, $\lambda_\odot = 139.^\circ6$ (2000.0).

Table 3 – Trajectory parameters.

Nr.	Date	Time	α	δ	V_g	h_{beg}	h_{end}	Q	SD_1	SD_2	m
2	Aug 11	$14^h48^m27^s$	52°.3	55°.7	57.3	112	103	4°.8	1'.15	0'.90	5.5
3	Aug 11	$15^h08^m58^s$	45°.6	57°.5	64.8	119	99	8°.5	0'.83	0'.96	1.5
6	Aug 11	$15^h20^m18^s$	44°.4	59°.1	62.7	114	103	5°.5	0'.93	0'.72	4.5
7	Aug 11	$16^h14^m58^s$	47°.0	57°.9	56.6	109	88	5°.8	1'.10	0'.94	4
10	Aug 11	$17^h09^m35^s$	48°.1	56°.1	61.0	96	90	25°.5	1'.10	0'.99	6.5
11	Aug 11	$17^h10^m06^s$	46°.1	56°.3	60.2	111	101	27°.3	0'.82	0'.67	6.3
12	Aug 11	$17^h25^m57^s$	45°.1	58°.1	59.5	111	97	63°.9	0'.98	0'.84	4.5
13	Aug 11	$17^h26^m22^s$	45°.2	58°.2	59.1	133	92	35°.0	0'.66	0'.91	0
15	Aug 11	$18^h05^m48^s$	46°.0	58°.7	56.7	113	86	30°.5	1'.00	0'.94	3.5
16	Aug 11	$18^h11^m02^s$	49°.6	55°.7	49.0	109	96	21°.5	0'.98	0'.89	6.5
17	Aug 11	$18^h19^m55^s$	49°.0	56°.0	57.8	108	95	19°.4	0'.93	0'.97	6.5
18	Aug 11	$18^h34^m06^s$	48°.5	57°.3	60.8	106	99	28°.9	1'.56	0'.95	7
21	Aug 12	$16^h11^m12^s$	50°.7	57°.0	54.7	122	93	4°.8	1'.02	0'.95	1.5
23	Aug 12	$16^h46^m22^s$	47°.6	57°.2	46.3	109	89	34°.3	1'.02	0'.96	2.5
24	Aug 12	$16^h49^m17^s$	49°.1	56°.9	58.0	99	90	29°.4		0'.85	6
25	Aug 12	$17^h00^m07^s$	48°.8	56°.2	52.4	107	99	30°.9	1'.33	0'.98	5
26	Aug 12	17^h02m49^s	46°.8	59°.0	63.2	115	96	31°.0	1'.21	0'.94	4.5
27	Aug 12	$17^h03^m46^s$	50°.3	56°.2	57.4	111	98	20°.7	1'.07	0'.93	5
28	Aug 12	$17^h06^m27^s$	48°.6	57°.9	57.0	114	98	19°.4	0'.90	0'.56	3.3
29	Aug 12	$17^h12^m59^s$	48°.5	58°.7	58.2	112	100	19°.0	0'.90	0'.61	4
30	Aug 12	$17^h19^m57^s$	47°.4	57°.8	58.1	123	97	18°.5	0'.93	0'.92	2.5
32	Aug 12	$17^h37^m12^s$	50°.3	58°.3	60.6	103	94	18°.6	0'.89	0'.90	6
34	Aug 12	$17^h46^m10^s$	51°.9	56°.3	48.7	120	99	21°.4	1'.49	0'.94	2
35	Aug 12	$17^h47^m12^s$	45°.1	57°.6	64.1	108	100	15°.4	1'.02	0'.94	5.5
36	Aug 12	$18^h08^m31^s$	44°.4	58°.3	65.2	110	97	12°.5	1'.07	0'.91	6
37	Aug 12	$18^h10^m57^s$	49°.4	58°.3	60.6	112	97	23°.8	0'.70	0'.62	5
40	Aug 12	$18^h20^m29^s$	52°.3	57°.8	59.3	101	96	20°.3	0'.94	0'.63	7.3
41	Aug 12	$18^h24^m42^s$	52°.5	57°.5	55.3	109	99	10°.6	0'.96	0'.95	3
42	Aug 12	$18^h29^m38^s$	45°.2	57°.1	60.6	119	92	34°.5	0'.79	0'.80	3
44	Aug 12	$18^h35^m23^s$	45°.5	57°.6	67.9	113	101	22°.1	0'.92	0'.92	4
45	Aug 12	$18^h39^m30^s$	47°.0	59°.0	62.4	111	98	22°.5	1'.10	0'.94	3
46	Aug 12	$18^h44^m36^s$	45°.8	58°.1	58.4	112	101	31°.0	0'.82	0'.92	6
47	Aug 12	$18^h56^m24^s$	46°.5	58°.3	59.0	118	94	22°.4	1'.12	0'.69	0.5
48	Aug 12	$18^h57^m58^s$	46°.0	57°.9	59.6	111	100	31°.2	0'.43	0'.70	5

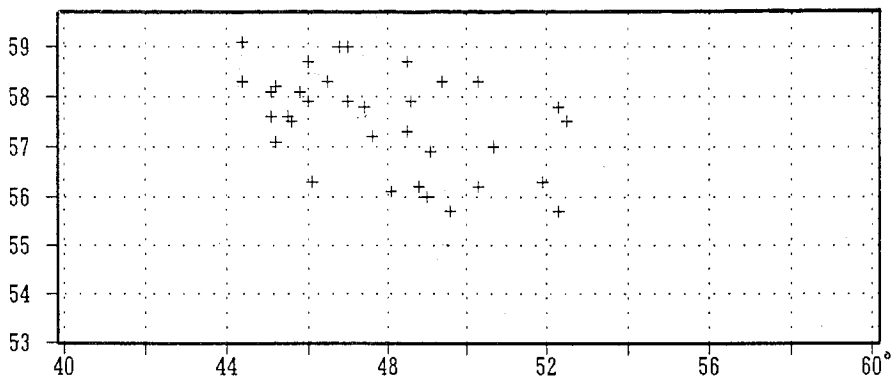

Figure 1 – Radiant point distribution of 34 meteors on August 11-12, 1993 (eq. 2000.0, α horizontally, δ vertically).

For August 11, 1993 (UT) we find $\alpha = 47°.2 \pm 2°.2$, $\delta = 57°.2 \pm 1°.2$, $\lambda_\odot = 139°.1$ (2000.0); and for August 12, 1993 (UT) we obtain $\alpha = 48°.2 \pm 2°.4$, $\delta = 57°.7 \pm 0°.8$, $\lambda_\odot = 140°.1$ (2000.0). The mean radiant point of the present TV observations agrees with the generally accepted value [2]. Sarma and Jones [3] observed 10 Perseids on August 12, 1983 (EST) with a TV setup. Their mean radiant point is $\alpha = 49°.3 \pm 1°.1$, $\delta = 55°.7 \pm 1°.2$, $\lambda_\odot = 138°.3$ (1950.0).

The determination of meteor velocities presents some problems. The mean velocity is $V_g = (58.6 \pm 4.5)$ km/s. The value of Sarma and Jones [2] is $V_g = (59.2 \pm 1.0)$ km/s. The Perseids' velocity is roughly definite. The correlation between velocity and magnitude is very weak, and is the same as between velocity and h_{beg} and h_{end}.

The Perseids are a high-velocity stream, so the beginning heights h_{beg} of the meteors are higher than for slower streams. The mean height is $h_{\mathrm{beg}} = (111.8 \pm 6.9)$ km/s, $h_{\mathrm{end}} = (96.4 \pm 4.3)$ km/s. We have plotted the h_{beg} and h_{end} of the TV meteors against apparent magnitude in Figure 2, which also shows full lines derived by correlation analysis. The correlation between h_{beg} and magnitude is considerably strong. The relation of h_{beg} and magnitude is according to the formula $h_{\mathrm{beg}} = -2.94m + 124.4$ (± 4.4). The correlation coefficient is 0.79, so there hardly exists a correlation between h_{end} and the magnitude.

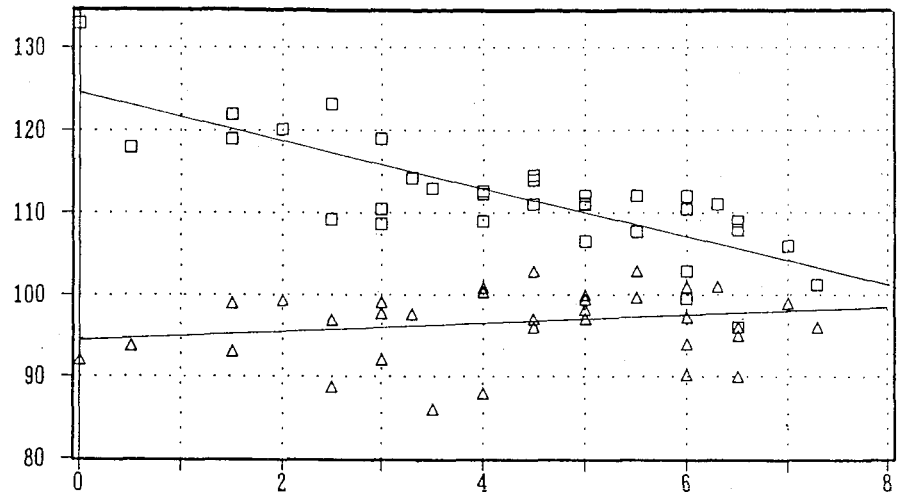

Figure 2 – The begin and end heights, h_{beg} (squares) and h_{end} (triangles), versus the apparent magnitude of the meteors.

The mean magnitude of the 34 TV meteors is 4.3. Figure 3 shows a histogram of the TV meteors' brightnesses observed by S. Suzuki only. 185 meteors were Perseids, and 337 were sporadic. The ratio of bright TV meteors in the Perseids is roughly similar to visual results.

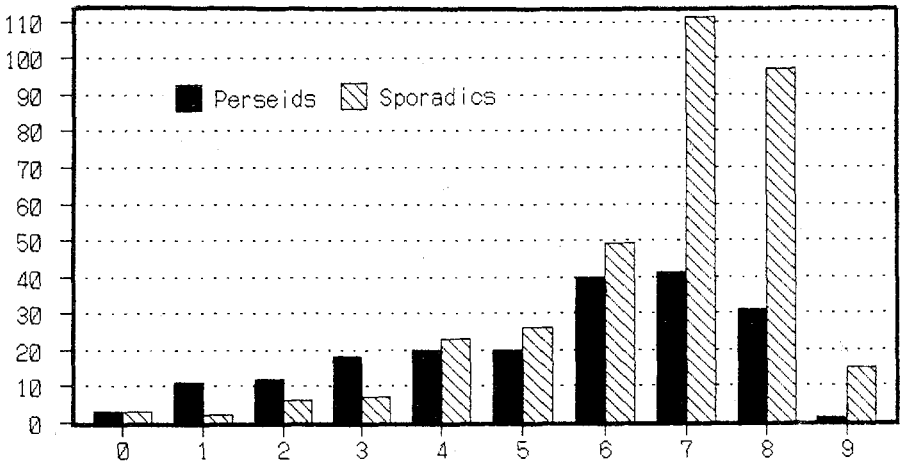

Figure 3 – Histogram of the apparent magnitude obtained from S. Suzuki only. There are 185 Perseids and 337 sporadics involved.

References

[1] K. Suzuki et al., "A New Minor Shower Belonging to the Coma Berenicid Complex?", *WGN* 22:2, April 1994, pp. 50–51.

[2] A.F. Cook, *IAU Colloq.* 13, NASA SP-319, 1973, p. 183.

[3] T. Sarma, J. Jones, *Bull. Astr. Inst. Czech.* 36:3, 1985.

The Forward Scatter Radar Method Using RDS

Peter Wright

A description of the author's system to observe radio meteors is described.

I have been forced to close down my observing station working on 75 MHz, a frequency used as an Aircraft Landing Navigation Aid, due to the fact that worldwide all transmitters have been modified and now have a power output too low for parasites like me to be of any use. This fact at first was rather annoying but it has turned out a very good thing that has forced me to think about the whole problem of forward scatter observations completely from scratch.

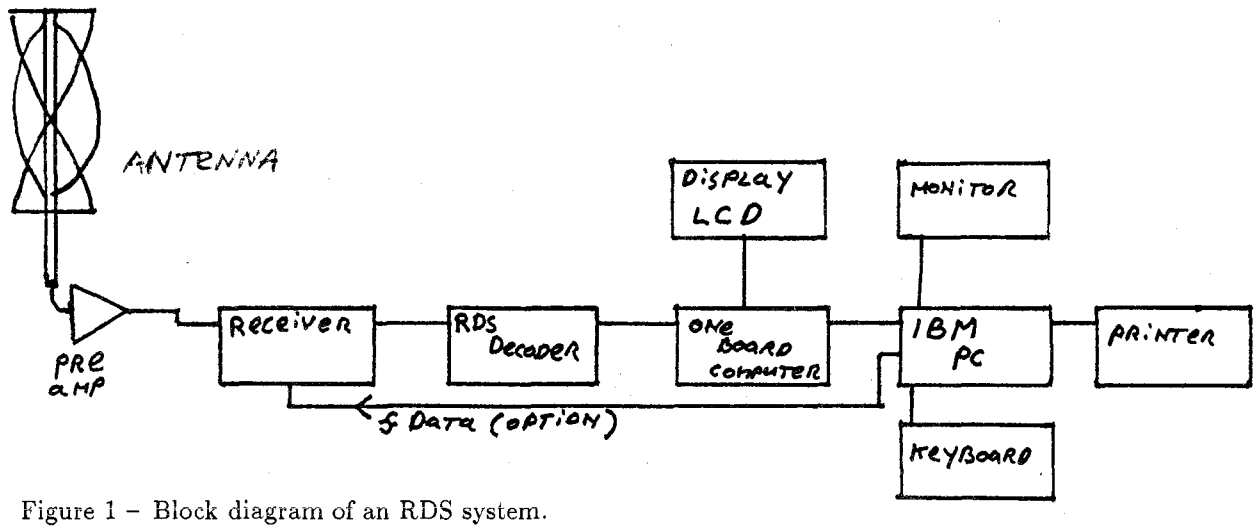

Figure 1 – Block diagram of an RDS system.

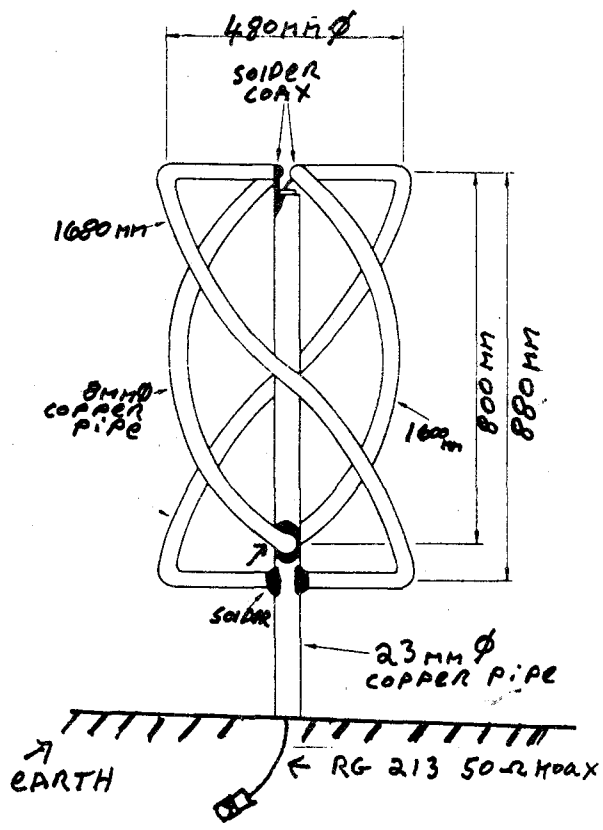

Figure 2 – The antenna.

I was browsing around a large music shop in Mannheim where I live when suddenly I noticed a new car radio which did not have the normal frequency display in MHz. Instead, in the LCD display was the name of the station. By closer inspection and a following conversation with a salesman, I understood that this new mode *RDS (Radio Data System)* was the answer to my forward scatter problem. (See Figure 1).

In fact it is a system that, used for radio meteor work, is far better than any system that I have ever dreamed of building. In the good old days, my system consisted of a crossed Yagi antenna, phased right circular polarization, preamplifier, receiver detector, DC amplifier, and chart recorder plus rolls and rolls of paper. The new unit looks totally different.

The antenna is a Quadriflar helix antenna used normally for space-Earth communication. This is needed because along the path with meteor reflections the incoming radio wave is no longer vertical or horizontal. The antenna is calculated for a frequency of 98.4 Mhz or middle of the FM radio band and is easily constructed using small bore copper piping.

The feed point at the top is almost always 50 ohm. However badly the antenna is constructed the quality of the right hand circular effect is as good as the antenna is bent. I advise the use of stiff cardboard and a pen to construct a master (see Figure 2).

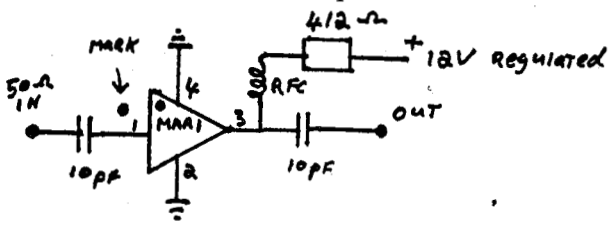

Figure 3 – A simple preamp DC - 1 GHz MAR1 chip (cost 15 DEM).

The RF Preamp is very simple or complicated whichever you wish. Either you build one using a ready finished IC amp, for instance the chip MAR1 which fits into any 50 Ohm system (see Figure 3) or you buy a finished high quality very robust one. A good source is the company SSB Electronic GMBH, Panzermacherstrasse 5, D-58644 Iserlohn, Germany, tel. +49-23716454.

It is well worth looking in their catalog. In general they are also very cheap for high quality. Ask for the current price of the LNA 3000 Preamp.

Any receiver can be used. The only thing is that the receiver should have a digital frequency display and the possibility to turn off the AFC (frequency tracking). Very important is that the receiver has the possibility that a connection can be made at the output from the FM detector (video signal) to be fed into the RDS decoder. A trick that helps is that this signal normally goes to the stereo detector. Find the input pin and that is where your coax cable is to be connected. The screen should be connected to ground.

The RDS demodulator, a very good design appeared in the magazine *Elektor* 2 (1991). This should be constructed in a tin screened box. The only hard thing about construction is the soldering of the S.M.D. decoder chip (see Figure 4).

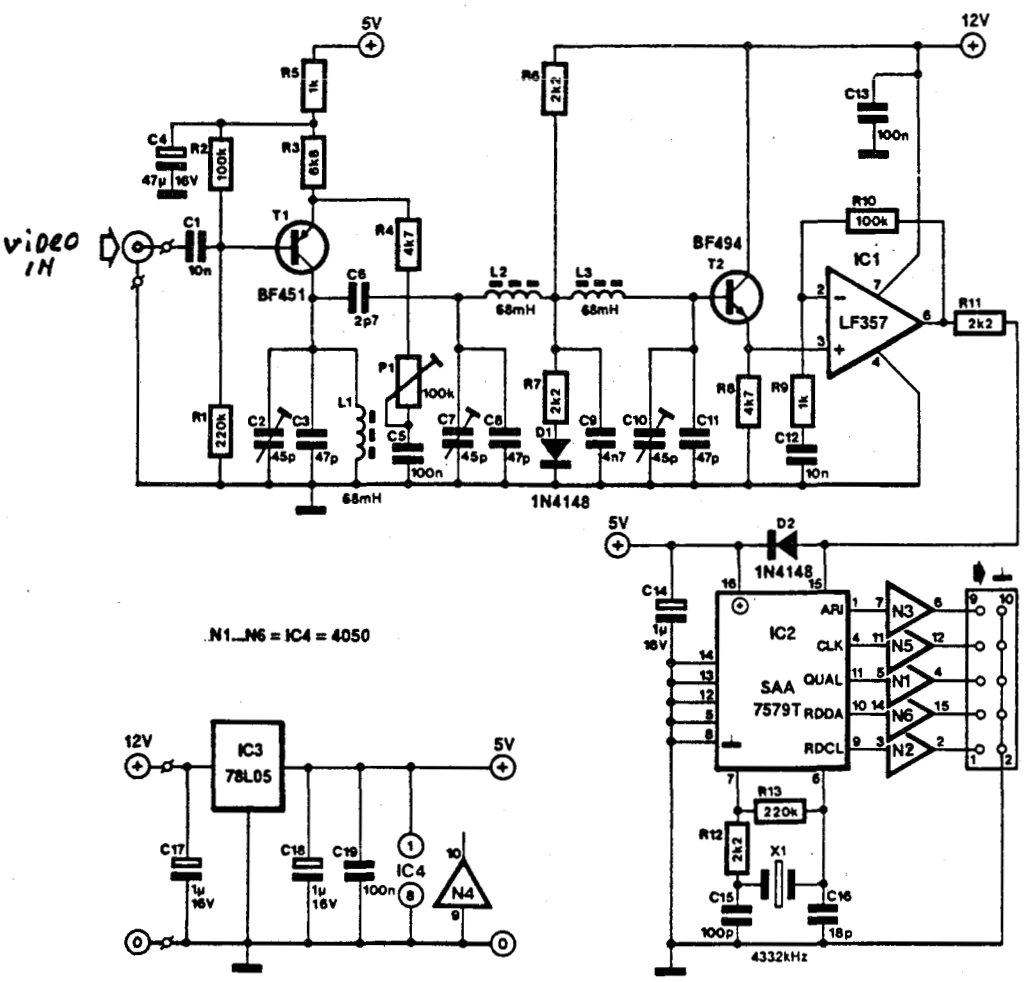

Figure 4 – The RDS decoder.

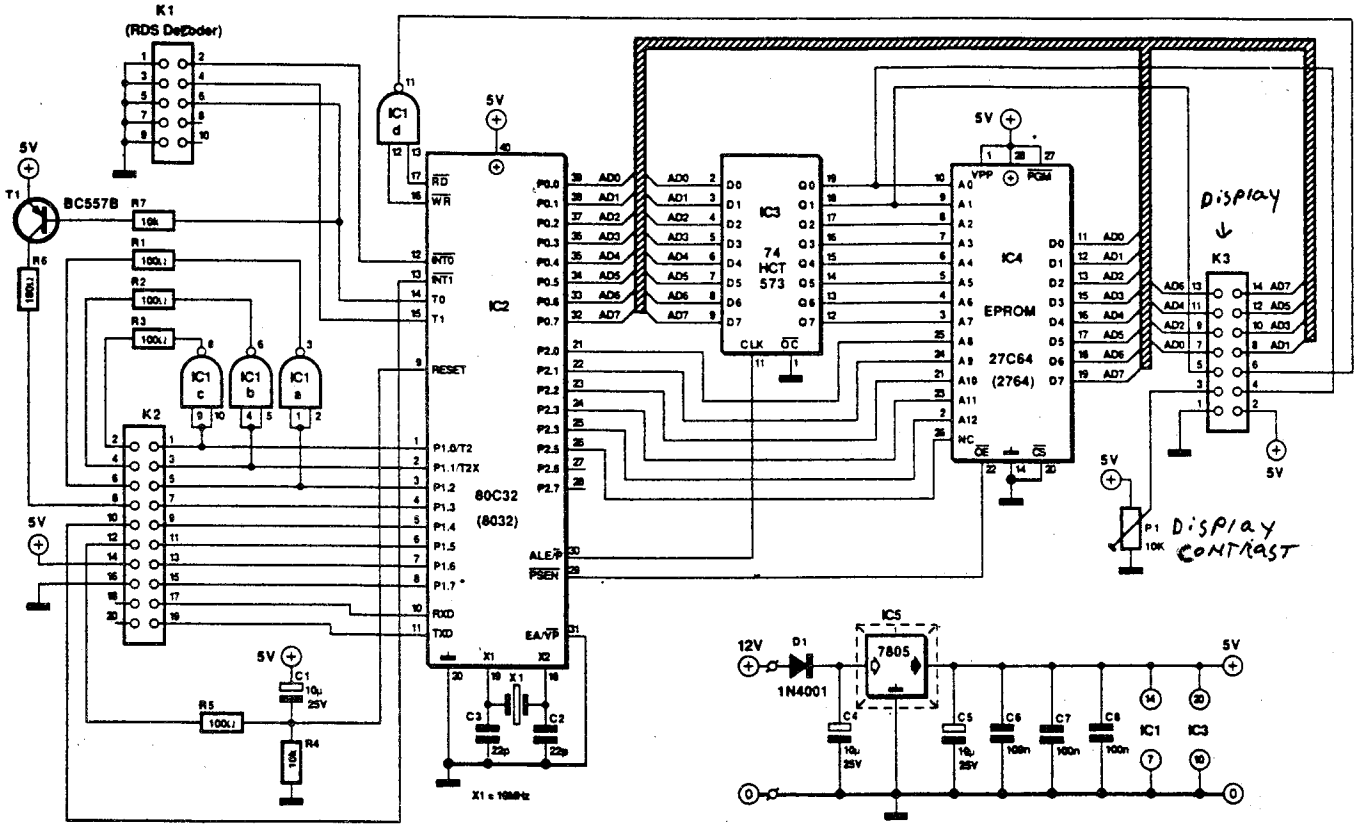

Figure 5 – The data computer.

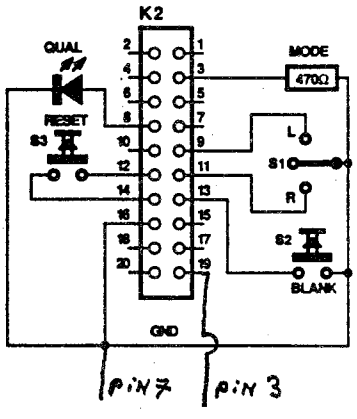

Figure 6 – The RS 232 port.

The 8032 epc or single board computer has the job of decoding the RDS data and giving it to an LCD display also giving the data to its serial port which can be connected to the computer (see Figures 5 and 6). Both units can be purchased in kit form from a company here in Germany. This is the best way; the kit is complete and very well put together and also cheaper than if you buy all the bits individually. The 2 kits are as follows: 910202, 8032 epc: RDS-decoder, 900060, for 150.44 DEM; 910203, RDS demodulator, 880209, for 87.17 DEM.

If interest is at hand the kits should be purchased soon, as I do not know how long they will be in stock. I said at the time of purchase that I would be writing this report in *WGN*, so please contact the company Geist Electronic GMBH, Hans Sachs Straße 19, D-78054 Villingen-Schwenningen, Germany, tel. +49-772036673. Ask also for a photocopy of the construction plans with your order.

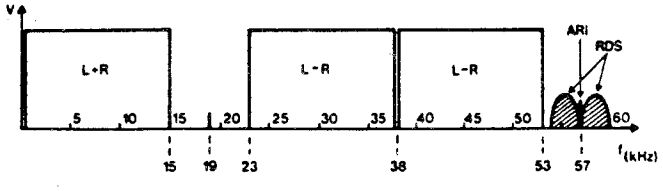

Figure 7 – The FM carrier signal.

Any computer can be used for data storage and processing. As no extra cards are needed the input is directly to one of the free serial ports. The computer waits for a packet data group from the decoder, stores the call sign, name, date, and time of the received signal by counting the data packets multiplied by 87.5 milliseconds per group, so giving the recombination time (see Figures 7 and 8).

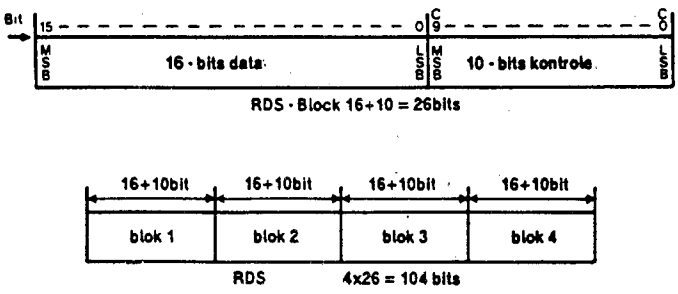

Figure 8 – The data format.

Now, what is very interesting is the fact that the position of my station is, e.g., 49°29′.12 N, 08°28′.35 E in Mannheim, Germany. All you have to do is read the call sign of the transmitter. Please note that this is not the name of the service; this call sign is noted in a book that is for Germany, giving the geographical position of every radio transmitter. The same information is probably in every country, so if you know of other information please let me know. A photocopy is available from me if anyone is interested. The book is also available. Its name is "Terrestrischer Rundfunk," reference FTZ17AB11;1993m and can be obtained from the Deutsche Bundespost, Fernmeldeamt Wiesbaden ZDV, Postfach 2429, D-65014 Wiesbaden, Germany. Thus the exact location of both receiver and transmitter are available.

The RDS system described above is in use since 1986 and is now widely in use all over the world.

One of the problems that I was worried about at the start was the danger of a so called packet crash which happens when one or more meteor trails or one or more transmitters are reflected causing double data arriving at the decoder (two people talking at the same time). This effect, however, does not often happen with a data speed of 1187.5 bits per second and, if it happens, that is the so-called "tough luck syndrome." I remember trying to distinguish from a 2-second bit of distorted audio if it was Italian or Spanish in the good old days with inky fingers, tape recorders and headphones.

I would be very happy to get in contact with anyone who is also interested in radio observations. My address is on the inside back cover.

Meteor Train Survey: Magnitude and Velocity Connection

George J. Zay

A meteor train survey is conducted from data obtained by my 1993 observations. This segment of the survey shows the trend of persistent train production as a function of magnitude and velocity from parent meteors.

1. Introduction

It has been well established that meteor train production is at least influenced by the meteor's magnitude and its velocity [1]. Other possible factors such as entry angles, chemical composition and shower membership are not being considered in this survey. I thought it would be interesting to see how my data would fall in place with accepted doctrine covering two simple factors. During my observations, I simultaneously monitor the radio on the FM band for future connections. It stands to reason that if my initial survey coincides with established results, then perhaps any other trend noted that involves radio monitoring with the same observations may have some validity also. Hopefully, this will be brought out in a future article with perhaps future years of data to add.

2. Survey parameters

I consider a total of 2873 eligible meteors from 44 nights arbitrarily spread throughout the year. This includes the Perseids, Geminids, Lyrids, and various minor showers and sporadics combined... basically a homogeneous bunch to look over. Those nights selected for consideration

were done while simultaneously monitoring the FM band radio (92.9 MHz). All observations took place at my Descanso observing site in Southern California in the USA (116°38′13″ W, 32°50′00″ N). Meteors of magnitude range from +5 to −3 were the only ones considered. There were far too few meteors brighter than −3 to be adequately utilized. Even within some magnitude classes, there were actually inadequate numbers of various velocity classes to continue. But these were still included. Meteor velocities were segmented into five divisions.

3. Results

My 1993 data are laid out below in Table 1. It is readily noted that the trend for magnitude/train relationships is classically displayed from magnitude +5 to 0. On the most part, the velocity/train relationship follows true also from magnitude +5 to 0. With a few failures to the expected trend (primarily amongst the slow and very slow velocities), the data tends to support what is expected.

Table 1 – Persistent trains showing their magnitude and velocity relationships.

Magn.	Percentage persistant trains					Total	Total	Percentage
	Very fast	Fast	Medium	Slow	Very Slow	Meteors	Pers. tr.	Pers. tr.
+5	0	0	0	0	0	99	0	0
+4	1.3	0	0	0	0	364	1	0.27
+3	4.5	1.6	1.4	0	0	685	16	2.3
+2	28.1	7.7	2.8	1.9	50	751	98	13.0
+1	41.5	18.7	1.8	8.3	0	481	104	21.6
0	65.8	38.1	5.1	11.1	0	249	100	40.0
−1	60.4	63.6	3.1	0	0	132	41	31.1
−2	65.7	75.0	13.8	0	0	80	34	42.5
−3	92.9	0	29.4	0	0	32	18	56.3
Tot.						2873	412	

Magnitude versus train:

From Table 1, it is clear that the percent of train production steadily increases from +5 to 0. From there, the percentage drops a little with the −1 magnitude class and again continues the gradual increase as brightness increases from magnitude −1 to −3. This slight discrepancy should be attributed to the lower number of meteors for that magnitude class. Surely with a greater sample of meteors, this slight anomaly would have been alleviated.

Velocity versus train:

Table 1, for the most part, shows the trend to produce less trains as meteor velocity decreases for nearly all magnitude classes. The few exceptions being those velocity classes of slow and very slow and magnitude classes of −1 through −3. Again, these discrepancies are a reflection of the fewer meteors to represent these categories.

4. Conclusion

Although a greater number of meteors would have been desired, what was available still sufficed to show the expected results. Simply put, based on these two factors alone, the brighter and the faster the meteor, the more chance for a persistent train to arise.

I intend to combine my 1994 data with this data and other years in the future. Hopefully I shall eventually have sufficient meteors to show the non-inhibited trend as expected. From there, branch out to seek other subtle trends and relationships as they pertain to radio signal durations versus persistent trains, radio signal durations versus visual magnitudes, and velocity versus radio signal durations.

Reference

[1] D.W.R. McKinley, "Meteor Science and Engineering", 1961, p. 139.

Observational Results

1993 Perseid Observations of the NVWS Meteor Section

B. Apeldoorn, F. Bettonvil, R. Gloudemans, N. de Kort, and U. Poerink

An overview is given of the results obtained by the Meteor Section of the Dutch *NVWS* during their 1993 Perseid campaign in Southern France.

Ten members of the Dutch *Meteor Section* set out on an extensive expedition in August 1993 to the Southern parts of France to observe the Perseids under far more favorable conditions than from the usually clouded and "washed-out" Netherlands.

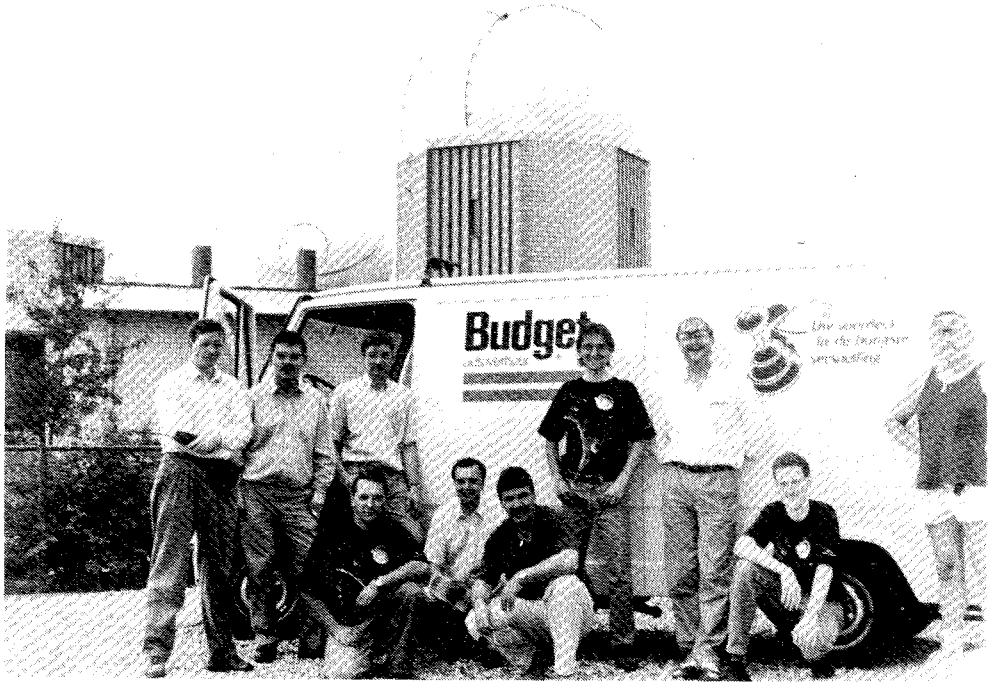

Figure 1 – The participants. From left to right: Urijan Poerink, Jeffrey Verbeet, Marc Neijts (sitting), Felix Bettonvil, Jacques Bouw, Niek de Kort, Serge ter Hall, Siem van Leverink, Roel Gloudemans, and Ben Apeldoorn.

With two buses, one full of equipment (and two persons) and the other mainly filled with eight persons, the long trip in a southerly direction started in the afternoon of Saturday August 7 from the Halley Observatory at Heesch (Figure 1).

The observation "hardware" mainly consisted of camera-batteries (in all more than 40 35-mm cameras) with synchronous rotating shutters; instruments for radio- and photometrical registrations; several quartz-clocks with large displays; tape- and cassette-decks for accurate timing and recording of visual data; and 4- and 10-inch equatorial driven telescopes. Sunday morning August 8, we arrived at our destination: the cottage "La Bastide Rose" at Salernes, our observing site. A day later, we set up a part of our photographic and data-recording equipment in a second, simultaneous station at Cabasse, 17 kilometers in a straight line south of Salernes. Although not optimal for accurate simultaneous measurements, this (rather small) distance offered the opportunity to make simultaneous meteor identification easier in the case of a real "storm" with many bright meteors appearing in small parts of the sky and in relatively short periods of time. The two stations together with several other stations formed a dense photographic network [1].

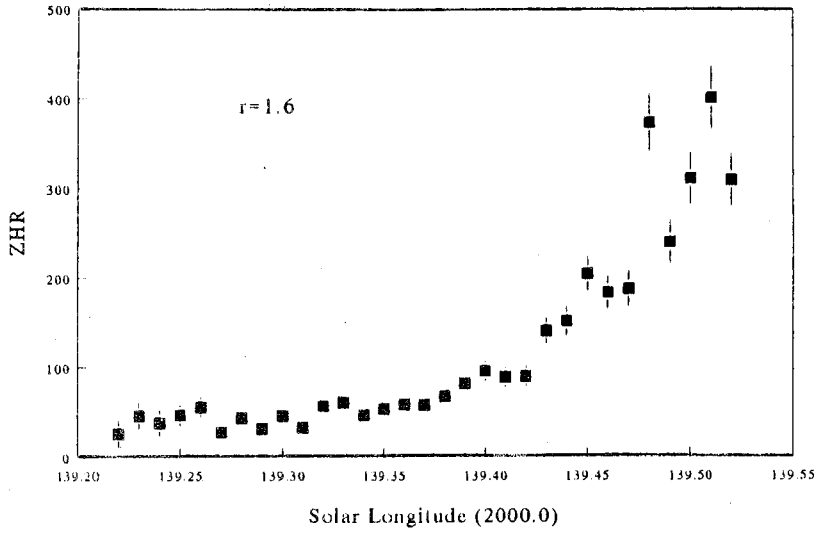

Figure 2 – ZHR diagram of the 1993 Perseid activity obtained from the observations at Cabasse and Salernes. The diagram is based on approximately 1200 Perseids during the night of August 11-12. Peak activity was recorded on $\lambda_{\odot} = 139°.48$ and $\lambda_{\odot} = 139°.51$.

Figure 3 – Five Perseid meteor trails around Ursa Minor eternalized during the early hours of August 12, 1993, local time, by the team at Salernes within 15 minutes exposure time. Photographs like this one make it difficult to determine times of appearance for the individual meteors from visual data.

Figure 4 – Fish-eye photograph taken from Cabasse (16 cm Nikkors) centered at 0^h10^m UT on August 12, 1993. The photograph on the front cover from Salernes was centered around the same time. Notice the striking resemblance. The short but strongly flaring trail, barely visible above at the center of the bottom edge of the picture, but clearly near the horizon on the front cover belongs to a magnitude −4 Perseid that appeared at $23^h49^m36^s$ UT on August 11. On the above photograph, three more meteor trails could be distinguished, two of which are very weak. The third one belongs to a fluctuating magnitude −3 Perseid that appeared near Lyra at $23^h44^m13^s$ UT.

As we already know, however, no real storm occurred. Nevertheless, we observed a very fine Perseid-display, thanks to excellent weather conditions in contrast with those in the Netherlands. To cut a long story short: of about 5.500 meteors, the required visual data were recorded. Handling of the visual data ended in a ZHR-curve of the new peak (August 11-12) as illustrated in Figure 2.

From telescopic observations we could not find an indication of enhanced activity at the position of the new peak, but nevertheless the regular maximum was observed clearly.

More than 700 meteors have been photographed, which is almost 30% of the whole, photographical "harvest" since August 7, 1953 (7 years after the foundation of our Meteor Section[1]), when the first meteor (a κ-Cygnid) was eternalized in the Netherlands by M. Alberts at Alkmaar. No less than at least half of that number was simultaneously photographed by our two stations: nearly ten times as much as in the past 40 years! See, for example, Figure 3 and 4.

[1] The NVWS Meteor Section was founded in 1946 as one of the working groups of the *Dutch Association for Astronomy and Meteorology (NVWS)*.

Figure 5 – The last 10 seconds of the 20-second persistent trail of a magnitude −10 Perseid was captured at Cabasse during a 1-minute exposure on Tri-X.

Furthermore, a number of Perseid meteors was observed by radio, and registered electronically (an image intensifier coupled to a PC). Of three bright meteors, the persisting trains were photographed, apart from their trails, by using a "persisting-train camera" ($f/1.8$, 50 mm). The persisting trail in Figures 5 was produced by a magnitude −10 Perseid that appeared on August 13, $2^h20^m48^s$ UT.

The large number of simultaneous negatives meant a tremendous amount of work. Each pair of negatives requires several hours for identifying meteors and a number of star trails, the actual measurements, data input, and final computations. This donkey work will become somewhat easier next fall, when a brand new, digital measuring device will become operational (thanks to the Committee of the *NVWS*), making it possible to feed coordinates directly into a PC program. Work is still ongoing, and we keep our spirits up!

Figure 6 – Friday, August 13, 1993, 6 sleepless nights and 5500 meteors later than Figure 1. All participants are assembled at a last exhibition of all the equipment used.

Reference

[1] C. ter Kuile, M. Langbroek, J. Kuiper, "The 1993 Perseids and Meteoroid Dust Cloud", *WGN* 22:2, April 1994, pp. 60–67.

1993 Orionids from the United Kingdom

Alastair McBeath

A summary of UK visual observations for the 1993 Orionids as seen by *JAS Meteor Section* members is presented.

1. Introduction

In the aftermath of August's excitement, September came as a considerable disappointment, bringing with it some very poor weather to the UK. October was a vast improvement, however, with 9 visual observers recording 504 meteors (including 198 Orionids and 48 Taurids) in 84 hours and 2 minutes. The observers providing these data were as follows:

Charlotte Bland, Marcus Buffrey, Shelagh Godwin, Richard Livingstone, Tony Markham, Tom McEwan, Graham Pointer, Ian Rigney, and Mike White.

2. Observations

Overall, observations were recorded on every night from October 13-14 to 23-24, with the exception of October 19-20, and some excellent meteors were seen, the most impressive a magnitude −7 fragmenting, blue Orionid fireball with an 11-second persistent train, noted at 2^h11^m UT on October 21-22. Mean ZHRs for the Orionids hovered around 10–15 between October 16-17 to 21-22, but were noticeably higher on October 20-21 at around 22^h UT. Highest activity on this night suggested a ZHR possibly around 25 or 30 between 2^h and 5^h UT. Low Taurid activity was seen for much of the month too.

Unfortunately, the October 17-18 Orionid outburst reported elsewhere (cfr. *WGN* 21:6, pp. 264–268) was not recorded by *JASMS* watchers, who were either not active at the critical time on that night, or reported little enhancement of Orionid rates. The few *JASMS* results from after midnight UT on October 17-18 came from either inexperienced observers, or were made under poor skies. Magnitude and train details for the reliably-seen Orionids and concurrent sporadics are given in Tables 1 and 2.

Table 1 – Global magnitude distributions for the 1993 Orionids and October sporadics.

Magnitude	-3^-	−2	−1	0	+1	+2	+3	+4	$+5^+$	Tot	$\overline{m}_{6.5}$
Orionids	4	4	3	18	19	34	17	3	0	102	1.99
Sporadics	1	0	3	3	31	43	47	24	1	153	3.08

Table 2 – Global train breakdown for the 1993 Orionids and October sporadics, giving numbers (N), percentages (%), and mean durations in seconds (D).

Magnitude	-3^-	−2	−1	0	+1	+2	+3	+4	Tot
N Ori	4	3	3	12	10	13	5	1	51
% Ori	100	75	100	67	53	38	29	33	50
D Ori	7.5	7.0	3.3	2.3	2.2	1.3	1.0	0.25	
N Spor	0	0	0	1	5	5	2	0	13
% Spor				33	16	12	04		08.5
D Spor				3.0	0.7	1.4	0.5		

Acknowledgment

As always, my thanks go to the *JASMS* observers noted above who provided the information for this report.

1993 Leonids in Kurdjali, Southern Bulgaria

Atanas Gavrailov and Roman Chakarov

An overview is given of 1993 Leonid observations from Southern Bulgaria. High activity was noted in the local morning of November 18.

Observations of this famous meteor shower are no tradition at the Astronomical Observatory in the city of Kurdjali. But following the predictions of the *ILW* for a possible increase in the activity connected with the return of comet Temple-Tuttle to perihelion, we decided to observe the Leonids. We also knew that the necessity of observational data is big, so this fact aroused us more. Unfortunately the weather conditions in Kurdjali could not be worse with thick clouds and snow on November 15, 16, and 17. Nevertheless, we had the opportunity to watch during the time of maximum, when in the early morning hours of November 18 the last cloud disappeared and the sky cleared up. The bright and trained meteors we saw, repaid our efforts and made us forget the extremely low temperatures (−8°−−10° C). We were astonished not only by the brightness of the Leonids but also by the number we could record with a limiting magnitude of around 5.3. The dawn of November 18 stopped our observation. Unfortunately, the post-maximum period was also covered with bad weather and clouds, and we could not follow the decrease of the very high activity we recorded on November 18. Table 1 shows the results of our observation.

Table 1 – Observational data of the 1993 Leonids from Kurdjali, Southern Bulgaria.

Observer	Period (UT)	T_{eff}	Lm	h_{rad}	Leonids
Atanas Gavrailov	0^h40^m–1^h40^m	1.00	5.3	45°	12
Roman Chakarov	0^h40^m–1^h40^m	1.00	5.1	45°	12
Atanas Gavrailov	2^h15^m–4^h00^m	1.25	5.3	65°	15
Roman Chakarov	2^h15^m–3^h15^m	1.00	5.1	65°	9

1994 Quadrantids from the United Kingdom

Alastair McBeath

A short review of data received for January, 1994, by the *JAS Meteor Section* is presented. Weather conditions and the presence of strong moonlight meant that only part of the Quadrantid maximum could be observed visually. Some preliminary radio data for 1994 January is also given.

1. Introduction

The opening days of 1994 provided several observers with the opportunity to get their meteor efforts for the year underway, and many clearly decided that in the wake of the excellent Geminid peak, an attempt to watch the Quadrantid maximum was still worthwhile, in spite of the waning gibbous Moon scheduled to ruin all but the early evening hours of January 3-4. At this time, the Quadrantid radiant is at its lowest point for the entire day, near the northern horizon from British sites.

Overall, nine observers contributed 20.94 hours of visual watches during January, most of this on January 3-4, for 232 meteors (175 Quadrantids). One photographer (Terry Holmes) made 2.37 hours of exposures at the Quadrantid peak as well, but recorded no trails, and one radio operator (Robert S. White) made 240 hours of near-continuous radio observations in two spells from December 31, 1993, to January 5, 1994, and from January 15 to January 20, 1994.

The visual observers, from the UK except where noted, were Peter Craven (Finland), Shelagh Godwin, Valentin Grigore (Rumania), Paul Haworth, Tony Markham, Tom McEwan, Ian Rigney, and George Spalding.

2. Visual Quadrantid results

With only short, mostly early evening, watches available for analysis, any conclusions reached must be very tentative, due to the large corrections for the considerable zenith distance of the radiant at such times, and the small number of meteors observed. Watches made later in the night often suffered from poor limiting magnitudes, thanks to the bright Moon, again rendering the data difficult to interpret. Table 1 contains details of the relatively few Quadrantid and January sporadic magnitudes from reliable, good sky condition sources. Insufficient train reports were received to permit a similar analysis for them, unfortunately. The mean limiting magnitude for the magnitude results was +5.7.

Table 1 – Global magnitude distributions for the 1994 Quadrantids and January sporadics.

Magnitude	-3^-	−2	−1	0	+1	+2	+3	+4	$+5^+$	Tot	$\overline{m}_{6.5}$
Quadrantids	2	1	1.5	15.5	21	11	15	3	3	73	2.3
Sporadics				2.5	6.5	4.5	3.5	7.5	2.5	27	3.4

Allowing for the problems noted above, the Quadrantid ZHR seems most likely to have been about 50–80 at about 21^h–22^h UT, when the majority of observers were active. The mean ZHR for this period was 65–70. It has not been practical to define the rate any more precisely than this with the current data set.

3. January radio data

The observations reported as raw ten-minute and hourly counts by Robert White were made using a simple dipole antenna facing eastwards, the receiver tuned to 67.4 MHz, to pick up mainly Budapest radio, broadcasting with a power of 100 kW. Graphs showing the data collected are given as Figures 1 and 2. The gap from 10^h to 17^h UT on January 2 was due to a printer fault.

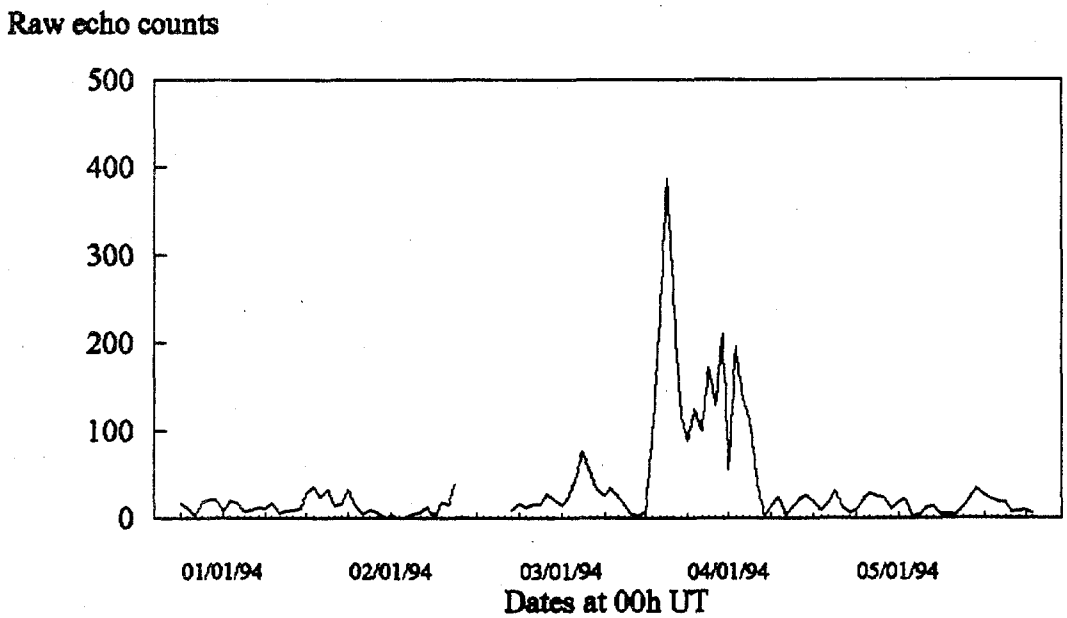

Figure 1 – Early January raw hourly counts of radio meteor echoes, made by Robert White.

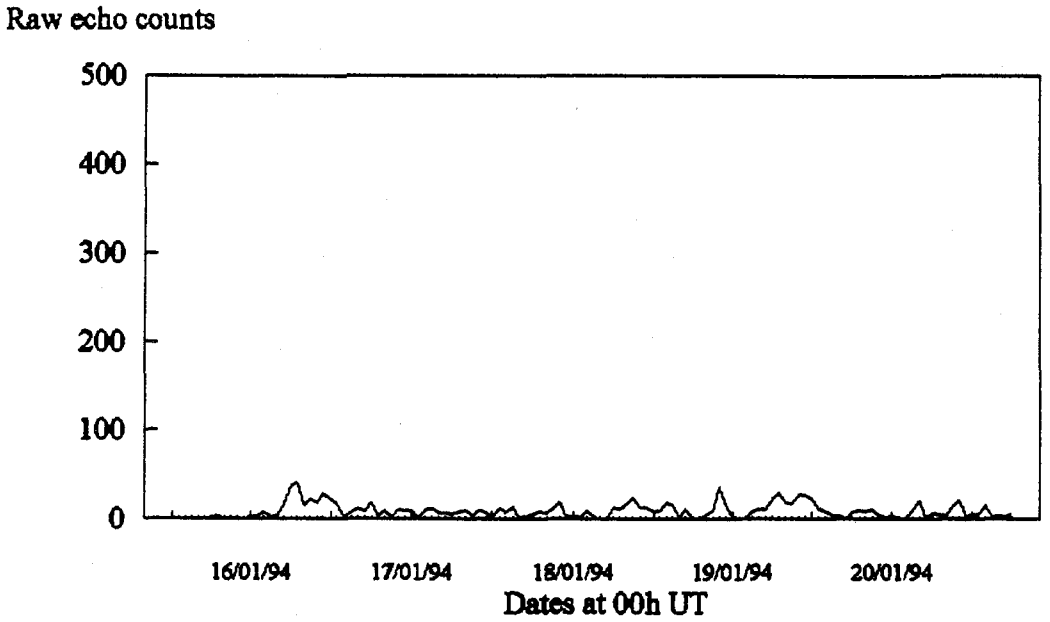

Figure 2 – Mid-January raw hourly counts of radio meteor echoes, made by Robert White.

Although only unprocessed hourly counts are shown, the effect of the Quadrantids on the rate detected is quite obvious, notably on January 3 and 4. It is useful to compare Figure 1 with Figure 2 made later in the month, since this latter almost certainly shows only the background sporadic activity. The peak hourly count of 387 echoes was recorded from 15^h–16^h UT on January 3, though this may not represent the true radio shower peak, since no account is taken of the radiant position or elevation at the time. Quadrantid rates were much in evidence between 13^h UT on January 3 till 5^h UT on January 4 from these results.

Curiously, few other UK amateur radio operators appear to have enjoyed much success for the Quadrantids in 1994, as Norman Fitch of the Radio Society of Great Britain, who collates reports on VHF and UHF propagation for the *RSGB*'s journal *RADCOM*, indicates that most radio amateurs enjoyed few opportunities to use the meteor scatter propagation mode during the shower this year. Whether this has resulted from simple bad luck or poor atmospheric conditions is not yet clear, however.

Acknowledgment

My thanks as always go to the observers who have contributed data for this paper, especially under skies as generally unhelpful as 1994 January's.

1994 η-Aquarids from Malta

Godfrey Baldacchino

An overview is given of the 1994 η-Aquarid observations by the *Malta Astronomical Society Meteor Group*.

The *Malta Astronomical Society Meteor Group* set off with its first observational project with a difference in May 1994. Target for the meteor watchers was the strong but largely neglected η-Aquarid annual meteor shower. Recognized as one of the strongest eight annual daytime meteor showers, its zenithal hourly rate statistic fluctuates widely between one source and another. This is testimony to the relatively sparse knowledge which has been documented about this

shower. Reasons for this are not difficult to find: the shower has its radiant practically on the celestial equator. While this means that the shower activity is actually visible from any location on the surface of the Earth, it is best seen by observers from southern latitudes which, at the time of the shower activity, are experiencing the winter season. Secondly, its appearance at a tolerable altitude above the observer's horizon (20°) coincides with the early morning and pre-dawn hours for Europe-based observers, possibly the most unlikely times for amateur meteor watching. In any case, such a strong and regular event is noticeable by its absence from the 1994 *IMO Calendar*, in spite of observing conditions particularly favorable during the latter period of activity.

Maltese observers are now probably the most southerly group of organized meteor watchers in Europe; we have therefore sought to exploit this comparative advantage by observing the 1994 return of this shower.

Meteor Group members carried out naked-eye observations (lasting some 30 hours in all) of the η-Aquarid shower from a variety of locations in Malta. The participating observers were as follows:

> Anna Baldacchino (**BALAN**), Godfrey Baldacchino (**BALGO**), Edwin Camilleri (**CAMED**), Franco Gatt (**GATFR**), Antoine Grima (**GRIAN**), Sandro Lanfranco (**LANSA**), and Umberto Mule Stagno (**MULUM**).

All 9 project nights (April 29-30 till May 7-8, 1994) were covered although there was appreciable lunar interference during the first 5 nights of the project. The magnitude distribution of the meteors seen is tabulated in Table 1, below.

Table 1 – Magnitude distribution of the 1994 η-Aquarids as seen from Malta.

Magnitude	−3	−2	−1	0	+1	+2	+3	+4	+5	Tot	$\overline{m}$
Aquarids	1	9	16	12	20	34	38	27	10	167	1.93
Sporadics	1	3	2	10	13	16	26	22		93	2.15

The low number of shower meteors seen per watch precludes a valid resort to magnitude ratio estimates for the calculation of meteor rates. The low shower altitude makes the resort to an altitude correction factor equally suspect since the multiplication factor is bound to be too high. Thirdly, the relatively poor skies also advise against using a limiting magnitude correction factor, since a high multiplier would necessarily have to be used. In view of the above circumstances, it was decided to complete an activity curve based on the relative performance of the Aquarid stream to its sporadic background. This was considered as the most valid approach since (1) it avoids utilizing limiting magnitude or altitude correction factors; (2) it is based on a series of observations held practically at the same time of the night (02^h00^m–04^h00^m UT); and (3) it is grounded on a database where the mean magnitude of shower and sporadic components differ by only 0.22 magnitudes (see Table 1 above). The technique, introduced to Maltese observers by former *BAAMS* and *JASMS* Director George Spalding, assumes a standard sporadic background. The activity curve is tabulated as Figure 1.

Assuming a standard (limiting magnitude of +6.5) sporadic background activity rate of 12 meteors per hour, the Aquarid rate on the night of maximum works out as $3.4 \times 12 \approx 40$ meteors per hour.

Noticeable also is a secondary maximum 2 nights after the first, on May 6-7, with a shower to sporadic ratio close to 2.0. This would be equivalent to a ZHR of 24 meteors per hour. This confirms the reports of a similar secondary peak by other observers, suggesting that the stream is actually an overlap of two different streams, the η-Aquarids (maximum on May 3) and the Halleyids (maximum on May 8). [1,2]

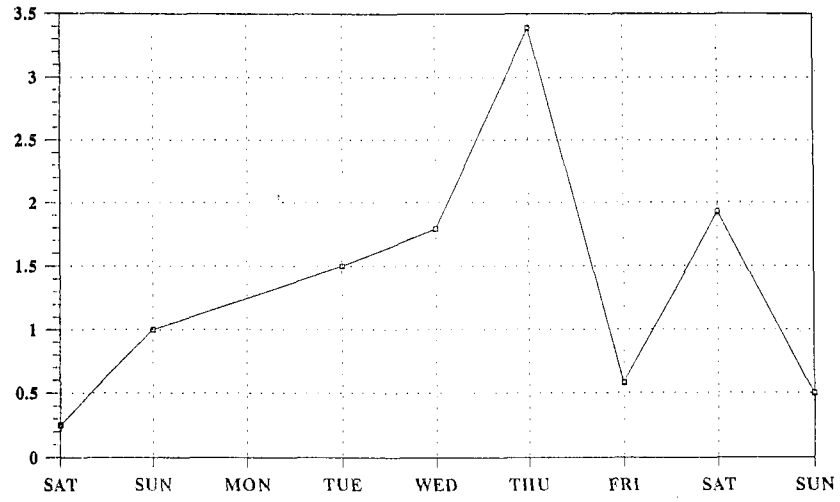

Figure 1 – Activity of the η-Aquarids as seen from Malta relative to the sporadic background, from Saturday, April 29-30, to Sunday, May 7-8.

References

[1] J. Wood, "Visual Observers' Notes: May–June 1994", *WGN* 22:2, April 1994, p. 3.
[2] M. Currie, "Telescopic Observers' Notes: May–June 1994", *WGN* 22:2, April 1994, p. 35.

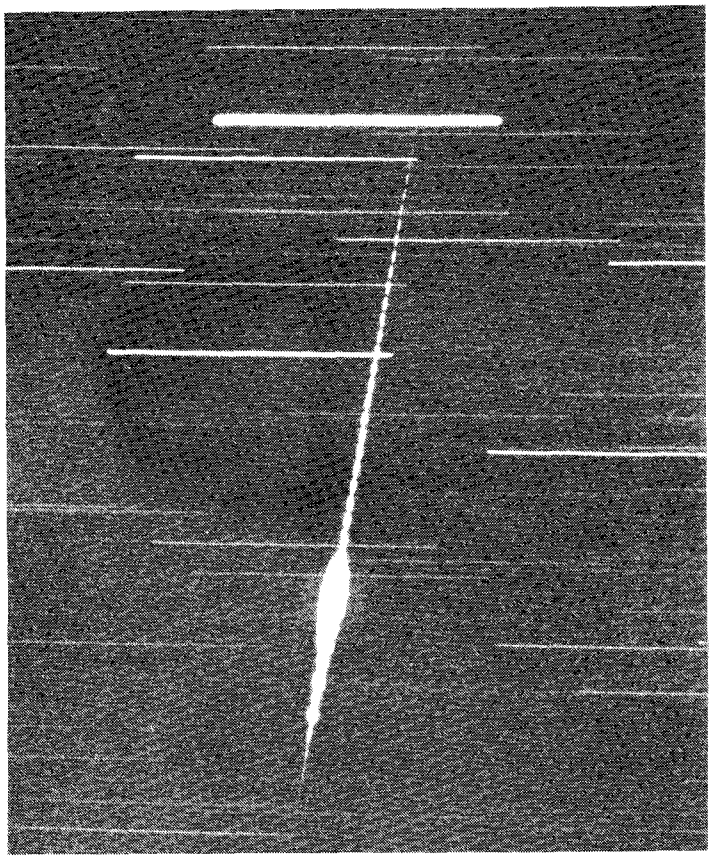

Magnitude -5 κ-Cygnid meteor photographed by Dutch observers in Rognes, Southern France, on August 13 at $21^h55^m20^s$ UT.

The International Meteor Organization

Council

President: Jürgen Rendtel, Gontardstraße 11, D-14471 Potsdam, *Germany*,
tel. 49 (331) 960 727, e-mail: rnl@babel.aip.de

Vice-President: Alastair McBeath, 25 West Park, Morpeth, Northumberld. NE61 2JP, *England.*

Secretary-General: Paul Roggemans, Pijnboomstraat 25, B-2800 Mechelen, *Belgium*,
tel. 32 (15) 41 12 25

Treasurer: Ina Rendtel, Gontardstraße 11, D-14471 Potsdam, *Germany*,
postal (giro) account number: 547234-107
post office code: 100 100 10 Postgiroamt D-10916 Berlin

Other council members:
Peter Brown, Dept. of Physics, Univ. of Western Ontario, London, *Ont., N6A 3K7, Canada*
Marc Gyssens, Heerbaan 74, B-2530 Boechout, *Belgium*
Ralf Koschack, Prof.-Wagenfeld-Ring 33, D-02943 Weißwasser, *Germany*
Graham Wolf, 66 Mein Street, Newtown, Wellington, *New Zealand*

Commission Directors

Visual Commission: Rainer Arlt, Berliner Straße 41, D-14467 Potsdam, *Germany*,
e-mail: 100114.1361@compuserve.com

Telescopic Commission: M. Currie, 25 Collett Way, Grove, Wantage, Oxon. OX12 0NT, *Engl.*,
e-mail: mjc@ast.star.rl.ac.uk

FIreball DAta Center: André Knöfel, Saarbrücker Straße 8, D-40476 Düsseldorf, *Germany*,
e-mail: starex@tron.gun.de

Photographic Commission: Jürgen Rendtel (ad interim)

WGN — The Journal of the International Meteor Organization and Observational Report Series

Editor-in-chief: Marc Gyssens, tel. 32 (3) 455 68 18, e-mail: gyssens@wins.uia.ac.be
fax: 32 (3) 820 24 21 (mention "for Marc Gyssens")

Editorial board: R. Arlt, D. Asher, M. Beech, P. Brown, M. Currie, M. de Lignie, W. Elford, G. Kronk, R. Hawkes, D. Hughes, J. Jones, C. Keay, R. Koschack, A. McBeath, D. Meisel, P. Pravec, J. Rendtel, M. Šimek, G. Spalding, I. Williams.

Addresses of authors not mentioned above

V. Velkov et al., Ul. G. Pejachevich 32, BG-9000 Varna, *Bulgaria*
M. Vints, Acacialaan 35, B-3583 Beringen, *Belgium*
L. Bellot, Inst. de Astrof. de Canarias, C/ Vía Láctea s/n, E-38200 La Laguna, Tenerife, *Spain*
J. Wood, 4 St. Kilda Road, Rivervale, *Western Australia 6103, Australia*
D. Steel, Anglo-Australian Observatory, Private Bag, Coonabarabran, *NSW 2357, Australia*
D. Artoos, Nattenhofstraat 74, B-2800 Mechelen, *Belgium*
P. Spurný et al., Astronomical Institute, CZ-25165 Ondřejov, *Czech Republic*
M. Beech, Astronomy Dept., Univ. of Western Ontario, London, *Ont. N6A 3K7, Canada*
S. Suzuki et al., 20-11 Ishika, Higashi-ohtomo-chou, Okazaki City, Aichi-ken 444, *Japan*
P. Wright, Ziethen Straße 97, D-68259 Mannheim, *Germany*
G. Zay, 3946 Paula Street, La Mesa, *CA 91941, USA*
B. Apeldoorn, Graaf Willem II-laan 30, NL-2355 BH Hoogmade, *the Netherlands*
A. Gavrailov, Astronomical Observatory, P.O. Box 134, BG-6600 Kardjali, *Bulgaria*
Godfrey Baldacchino, "Sirius" Triq Il-Migbha, Marsascala, *Malta*

Do not miss it!
International Meteor Conference 1994
Belogradchik, Bulgaria, September 22–25, 1994

The 1994 International Meteor Conference will take place in Belogradchik, in the northwestern part of Bulgaria, in most beautiful surroundings.

It will be the first *IMC* in the Balkans, and we hope that it will be easy for people from East European countries to participate. We cordially invite you to register for this meeting!

But do not hesitate any longer! In Belogradchik, there is overnight accommodation for only 60 persons, limiting the number of participants.

Contact the local organizers immediately if you do not want to miss this unique event! (See inside this issue.) It would be a pity if you could not participate in the 1994 *IMC* just because you were late!

As usual, the *IMO* will publish proceedings of this *IMC*.

Available now: Proceedings
International Meteor Conference 1993
Puimichel, Southern France, September 23–26, 1993

The proceedings of this International Meteor Conference are available now! The book contains articles about various fields of meteor astronomy—almost entirely covering the conference.

Included are: visual and photographic observations, radio meteor work, telescopic and video observations, new techniques in meteor observation, data processing, investigations on meteorite events in the past, meteor physics and the International Meteor Organization itself.

These proceedings are published by the *International Meteor Organization* and can be ordered at only 12 DEM per copy (surface mail delivery). Note that the proceedings were included in the registration fee for the participants of the 1993 *IMC*; they should have received their copy with the April issue of *WGN*. Non-participants can order these proceedings in the same way as paying for *WGN*!